



# **Air pollution emissions from diesel trains in London**

**Prepared for London boroughs of Ealing and Islington under Defra air quality grant reference 334d2011**

July 2014

Gary Fuller, Timothy Baker, Anja Tremper, David Green, Anna Font, Max Priestman, David Carslaw, David Dajnak, Sean Beevers,

Environmental Research Group

King's College London

<b>Title</b>	<b>Air pollution emissions from diesel trains in London</b>
--------------	---

<b>Customer</b>	<b>London boroughs of Ealing and Islington – Defra AQ grant.</b>
<b>File Reference</b>	AIRQUALI\LONDON\LA\EALING\Railways Emissions Project

<b>Report Number</b>	
----------------------	--

Environmental Research Group  
 King's College London  
 4th Floor  
 Franklin-Wilkins Building  
 150 Stamford St  
 London SE1 9NH  
 Tel 020 7848 4044  
 Fax 020 7848 4045

	<b>Name</b>
<b>Lead Author</b>	Gary Fuller, David Dajnak, David Carslaw
<b>Reviewed by</b>	David Dajnak, David Carslaw
<b>Approved by</b>	David Carslaw

## Table of Contents

1	Summary.....	4
2	Introduction .....	5
3	Project aims .....	7
4	Materials and Methods .....	7
4.1	Measurement locations.....	7
4.2	Measurement methods .....	11
5	Results .....	12
5.1	Gas and particle concentrations.....	12
5.2	PM composition. ....	14
6	Analysis of PM composition and local sources .....	15
7	Analysis of NO <sub>x</sub> , NO <sub>2</sub> and PM <sub>10</sub> concentrations along with CO <sub>2</sub> .....	20
7.1	Preliminary considerations .....	20
7.2	Emissions considerations.....	22
7.3	Linking with measured pollutants including CO <sub>2</sub> .....	23
8	Emissions and dispersion modelling .....	31
8.1	Method .....	31
8.2	Model results .....	34
9	Conclusions.....	41
10	Recommendations for further research .....	43
11	Acknowledgments .....	44
12	References .....	45

## 1 Summary

Current modelling based on the London Atmospheric Emissions Inventory (LAEI) suggests that diesel trains may be responsible for breaches of the NO<sub>2</sub> annual AQ Objective up to 200m either side of the Paddington mainline through residential areas of Ealing with concentrations predicted to be more than 50% higher than the Limit Value. Measurement sites were installed alongside the Paddington and East Coast Mainline to test the modelled predictions and to derive new emissions factors.

Real world measurements did not support the modelled predictions and a clear pollution signal from the diesel trains was difficult to detect. This was the case for regulated gaseous pollutants, airborne particles and also for metal particles from train track wear. Given that diesel trains emit similar types of pollutants to diesel traffic, it is possible that London's traffic masked a clear signal from the trains; however, it is clear that diesel trains do not make a large contribution to local air pollution concentrations. This finding has clear implications for local air quality management priorities in Ealing and Islington and other local authorities with diesel train lines.

The absence of a clear signal from train emissions prevented the derivation of new emission information on diesel trains exhaust as originally intended. Instead, alternative information about emissions from UK diesel trains (Hobs and Smith, 2001) was used to adjust the emissions information in the LAEI and the resulting ambient pollution concentrations were modelled. The new results showed good agreement with measured concentrations.

Without this measurement study large resources could have been expended to abate pollution emissions from diesel train lines that pass through urban areas. The findings of the project also raises important issues for the use of emissions information to predict ambient air pollution. The amendment or introduction of emission sources needs to be verified against real-world measurements before being used in air quality and policy assessments.

The pollution concentrations from diesel trains within enclosed stations were not within the scope of this project.

## 2 Introduction

Modelling based on the London Atmospheric Emissions Inventory (LAEI) suggests that diesel trains may be responsible for breaches of the NO<sub>2</sub> annual AQ Objective up to 200 m either side of the Paddington mainline through residential areas of Ealing. Figure 1 and Figure 2 show the model annual mean NO<sub>2</sub> concentration in London for 2010 using the 2010 London Emissions Inventory. These modelled predictions show that the annual mean concentrations close to the Paddington Mainline exceed those close to the nearby arterial roads; the A40 to the north and the M4 to the south. More importantly the emissions from the Paddington Mainline gave rise to larger area exceeding the EU Limit Value when compared to these arterial roads and residential concentrations up to 60  $\mu\text{g m}^{-3}$ .

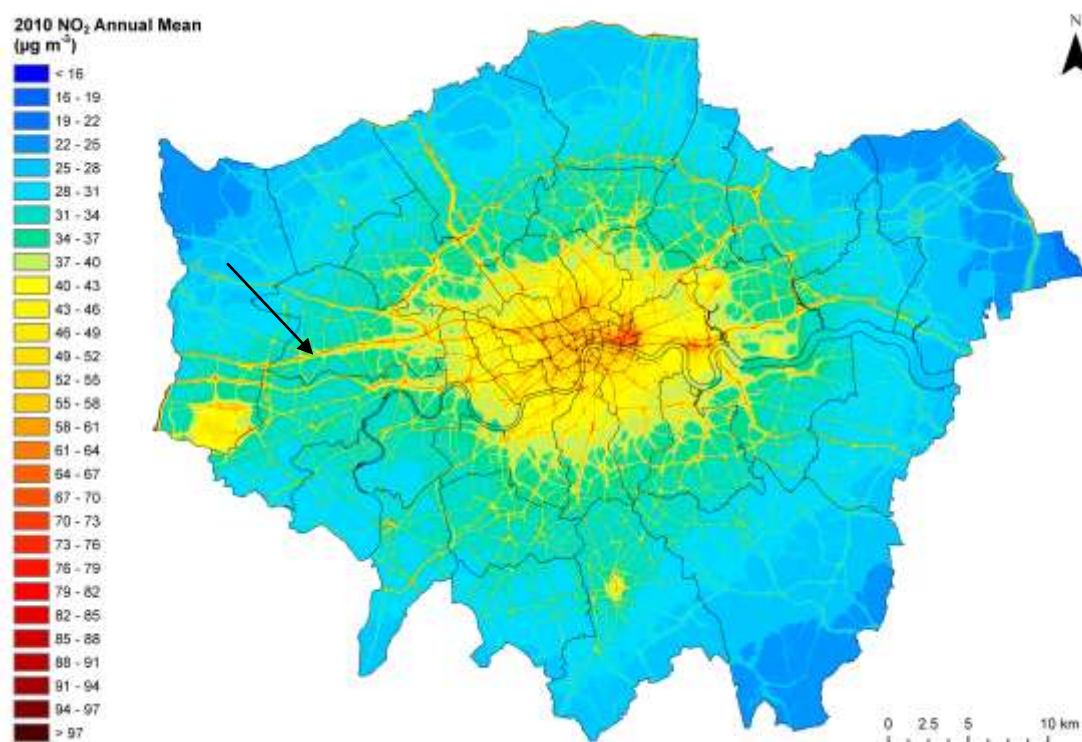


Figure 1 Modelled annual mean NO<sub>2</sub> concentration in London for 2010. Arrow indicates the Paddington mainline. Areas shaded in yellow and to red exceed the EU Limit Value of 40  $\mu\text{g m}^{-3}$ .

There are similar concerns about the more limited diesel traffic on the East Coast Mainline in residential Islington as shown in Figure 2, although here the line gives rise to lower concentrations when compared with many arterial roads in the area and the line is difficult to see against background concentrations within Islington although it is more apparent as the line enters lower emission areas in Haringey to the north.

The current LAEI estimates train emissions using energy dependent emission factors in part derived from work undertaken by the Danish Technical University (Jorgensen and Sorrenson, 1995, Bek and Sorenson 1999). This approach was first instigated in the LAEI for 2008, designed to improve upon the simpler g/km emissions approach used in the LAEI 2005 and before.



*Figure 2 Modelled annual mean NO<sub>2</sub> concentration for 2010. Left panel shows west London with the Paddington Mainline indicated by an arrow. The right panel shows inner north London with the East Coast Mainline indicated with an arrow. Areas shaded in yellow and to red exceed the EU Limit Value of 40 µg m<sup>-3</sup>.*

However, current limited ambient measurements suggest that the modelled predictions exceed ambient concentrations. There is therefore a risk that action planning based on current modelled concentrations may be disproportionate.

Whilst many studies support the emissions of air pollution from road traffic sources there is practically no information on air pollution from trains. The majority of available studies have focused on either in-train exposure or PM in underground environments (Gerhig et al. 2007).

A series of experiments in Switzerland sought to measure particle emissions from electric trains. Here the measurement strategy involved installing sampling sites at different distances along a perpendicular transect from 10 to 120 m away from a busy rail line (Gerhig et al 2007). PM concentrations were dominated by Fe particles which added around 1 µg m<sup>-3</sup> to the local PM concentrations at 10 m from the railway line. Lesser concentrations of Cr, Cu and Mn were also found; consistent with track and conductor wear. At 120 m from the tracks, the concentration PM from the railway was around 25% of that measured at 10 m distance. In the UK Burchill et al (2011) measured particle number emissions from diesel trains using the West Coast Mainline through Lancashire showing that emissions were well mixed in the wake of trains; largely due to their speed and length. Swiss studies also found that around 60 to 70% of the metal particles from the railway were in the PM<sub>2.5-10</sub> size range (Bukowiecki et al 2007), consistent with these coming from wear processes. Other studies in Switzerland also found Ca and Al particles close to electric railways consistent with track bed wear (Lorenzo et al 2006).



A limited set of test-bed measurements Sawant et al (2007) have explored  $\text{NO}_x/\text{NO}_x$  emissions from US diesel locomotives. These were found to be greatest at low engine loads, decreasing as load increased, but were constant for all settings above  $\frac{1}{4}$  throttle. PM emissions showed a similar pattern with respect to engine throttle settings, however, emissions at idle were dominated by organic particles with elemental carbon being dominant as the engine throttle was increased. A single study in Australia has sampled diesel train exhaust emissions from very large freight trains crossing otherwise pristine environments (Johnson et al 2013); however, these measurements are unlikely to provide information directly relevant to the passenger train types using London's railways. Emissions factors from UK diesel trains were assembled by Hobson et al 2001 based, for the most part on data assembled by the London Research Centre in the late 1990s. This provides  $\text{g km}^{-1}$  emissions for many of the train types still in use around London today.

### 3 Project aims

The project had the following aims:

- Improve the accuracy of the current modelled predictions that indicate breaches of the AQS  $\text{NO}_2$  annual objective 200 m either side of the Paddington mainline;
- Use measurements from two continuous monitoring sites to derive new  $\text{NO}_x$ ,  $\text{NO}_2$  and PM emissions factors for diesel locomotives and multiple units that use the Paddington and East Coast mainlines, including differences between accelerating and cruising trains;
- Determine the cause of any measured short-term peaks in  $\text{NO}_2$  from railway emissions;
- Differentiate between exhaust and wheel/track wear metal PM emissions from trains and also to estimate track/wheel/conductor wear PM emissions from electric trains.

## 4 Materials and Methods

### 4.1 Measurement locations

Air pollution was measured at two trackside locations in suburban London; one adjacent to the Paddington Mainline, near the Southall train station in Ealing (Ealing 12); and the other on the East Coast Mainline in Islington (Islington 6).

The study was undertaken over a 19 month period; from January 2012 to August 2013. During this time  $\text{NO}_x/\text{NO}_2$  and  $\text{PM}_{10}$  particulate was measured at both railway monitoring sites.  $\text{CO}_2$  measurements were also carried out to enable the calculation of emissions factors based on diesel fuel burn. These measurements were undertaken alongside the Paddington Main Line from February to September 2012 and then along site the East Coast Mainline September 2012 until April 2013. Particle speciation campaigns were also undertaken at Ealing 12 in early 2012 and then at Islington 6 during early 2013. During these times  $\text{PM}_{10}$  was sampled onto filters for subsequent laboratory analysis for particulate metals and real time measurements of equivalent black carbon (BC) were also made.

As pointed out by Lenschow et al (2001), the pollution concentrations measured at a location are the combination of those from sources with very different spatial scales; local, city background and regional. Background measurements were therefore undertaken to quantify the local sources distinct from those from the city background and region. It was assumed that these background sites captured the combination of city background and regional sources that were prevalent at the railway monitoring sites. The measurement sites are detailed below.

### ***Paddington Mainline – Ealing 12***

The Ealing 12 monitoring site was installed around 10 m north of the Paddington Mainline just west of Southall Station in April 2011. The site operated for the period of the study and continued to measure  $\text{NO}_x/\text{NO}_2$  and  $\text{PM}_{10}$  until closure in January 2014. The site was located on a residential road with no through traffic as shown in Figure 3.

Diesel trains used all four tracks close to the monitoring site. The southerly pair of tracks were used for High Speed Trains (HST) to the west of England and Wales. The north pair of tracks were used by local trains including the diesel powered class 146 passenger trains and freight. A small number of class 180 diesel trains run along with HST services on the southern tracks. These total five trainsets (Charles Buckingham, personal communication).



*Figure 3 The Ealing 12 monitoring site. The left hand panel shows an aerial view and the right hand panel shows the location of the monitoring site as seen from the nearby road bridge looking west.*

### ***East Coast Mainline – Islington 6***

The Islington 6 monitoring site was installed in March 2007 and continues to operate at the time of writing. The site measures  $\text{NO}_x/\text{NO}_2$  and  $\text{PM}_{10}$  and is located around 10 m from the East Coast Mainline, in the grounds of an environmental education centre as shown in Figure 4. The site is not close to a road but occasional rail maintenance vehicles pass close by to access the track to the north. The tracks immediately next to the monitoring site are used by electric trains only. The elevated lines further east are used by a mixture of train types including diesel powered HST services to the north of England and Scotland. The environmental education centre is heated by a modern biomass boiler located 20 m east of the monitoring site.





*Figure 4 The Islington 6 monitoring site. The left hand panel shows an aerial view and the right hand panel shows the monitoring site itself looking west.*

### **Background monitoring sites**

Three background monitoring sites were used to support the analysis. Details of these monitoring sites can be found at [www.Londonair.org.uk](http://www.Londonair.org.uk).

- Ealing 7 (Southall) – Located around 900 m from Ealing 12 and around 600m from the railway line, this long-term monitoring site measured  $\text{NO}_x$  /  $\text{NO}_2$  and  $\text{PM}_{10}$ .  $\text{CO}_2$  measurements were also made at the site for the same time period as  $\text{CO}_2$  measurements were made at Ealing 12.
- North Kensington – Located in inner London this is a background supersite for London. Background BC measurements were made at the site as part of Defra funded networks. Daily measurements of  $\text{PM}_{10}$  metals were also available at the site during 2012 as part of the NERC funded ClearLo project and the MRC-NERC funded Traffic project.
- Tower Hamlets 5 (Victoria Park) – Located immediately west of the Olympic Park and 5.4 km from Islington 6, this site measured  $\text{NO}_x$  /  $\text{NO}_2$ ,  $\text{PM}_{10}$  from July 2012 onwards.  $\text{CO}_2$  measurements were also made at the site for the same time period as  $\text{CO}_2$  measurements were made at Islington 6.

### **Diffusion tube monitoring sites**

Continuous measurements were supplemented by  $\text{NO}_2$  diffusion tubes. Figure 5 shows the location of  $\text{NO}_2$  diffusion tubes. These were deployed in pairs on the north and south side of the railway line. The north diffusion tube on the west of Figure 5 was located approximately 20-25 m north west of the continuous monitoring site at Southall. Figure 5 shows the diffusion tube sites around the East Coast Mainline. These were located in a densely resident area to between the East Coast Mainline and the electric line to Moorgate.

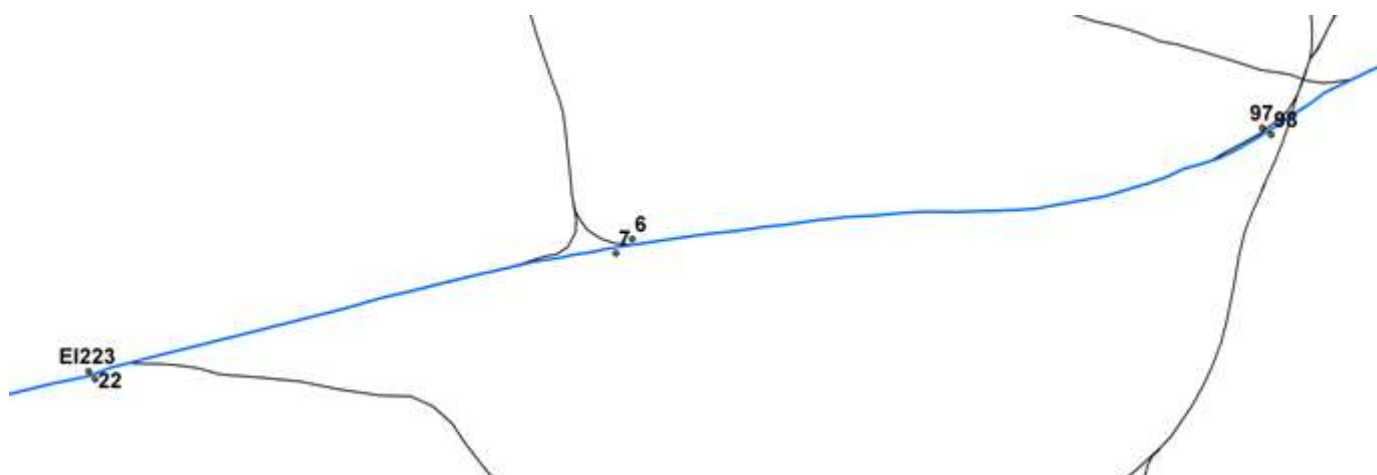


Figure 5 The Ealing 12 (EI2) and six diffusion tube sites (6, 7, 22, 23, 97, 98) locations alongside the Paddington mainline (blue). Other rail lines are shown in black. Pairs from west to east are; Southall, West Ealing, Acton. EI2 and diffusion tube 22 are located ~20-25m apart.

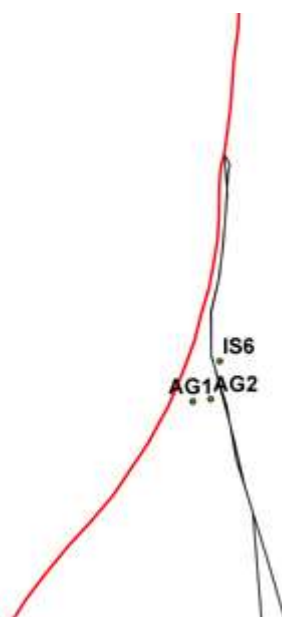


Figure 6 LAQN site IS6 and two diffusion tube sites (AG1, AG2) locations alongside the East Coast Mainline

## 4.2 Measurement methods

Long-term measurements of  $\text{NO}_x/\text{NO}_2$  were made by chemiluminescence using a variety of equipment types. These were calibrated two-weekly using gas standards with traceability to national meteorological standards.  $\text{PM}_{10}$  measurements were undertaken using the Tapered Element Oscillating Micro-balance method (TEOM, Thermo).  $\text{NO}_x/\text{NO}_2$  and  $\text{PM}_{10}$  measurement equipment were audited twice yearly by the National Physical Laboratory who hold UKAS accreditation for these tests. It is well known that the TEOM's elevated sample temperature causes poor sensitivity to semi-volatile particulate such as nitrate and some organics. TEOM measurements were therefore corrected to EU reference equivalence using the Volatile Correction Model (Green et al 2009).

$\text{CO}_2$  measurements were undertaken using LiCor-820 instruments. These were calibrated with traceable  $\text{CO}_2$  standards.

PM sampling for metals in  $\text{PM}_{10}$  was undertaken onto GN metrical (mixed cellulose esters) filters (Pall, USA) using Partisol Samplers (Thermo, 2025). Flow rates were calibrated using a flow meter (Bios) with traceability to national metrological standards. Post sampling, laboratory and travel blank filters were first digested in a 1:2 mixture of perchloric and hydrofluoric acid; using facilities at Royal Holloway University of London, to ensure that all chemical components were available for the inductively coupled plasma mass spectrometer (ICP-MS) analysis at King's. ICP-MS outputs were post processed using specialist software to derive calibration curves (X-genline, NPL) with additional protocols to account for analytical drift using standards within each analytical batch and blank filter measurements for each analyte. Uncertainty for the daily metal measurements was estimated to be 8.9% ( $K=2 \sim 2 \sigma$ ) including both analytical and sampling uncertainties

BC measurements were undertaken by measuring the real-time infra-red absorption of particles sampled onto quartz filters using aethalometers (Magee Scientific) and using the aethalometer default BC mass absorption coefficient of  $16.6 \mu\text{g m}^{-2}$  at 880 nm. Whilst sufficient space was available at Islington 6 to install a full size AE21, the small size of the monitoring cabin at Ealing 12 meant that the smaller AE31 had to be used. These instruments required different operational approaches.

- AE21 – The AE21 is designed for unattended operation and procedures here mirrored those on the Defra black smoke network. Particles are sampled onto a filter tape which was advanced automatically as each sampled filter spot became too loaded for the measurement to continue. In common with other BC measurement methods, light scattering and filter loading effects induce a non-linear relationship between the light absorption and the BC concentration. Measurements using the AE21 were corrected using the method suggested by Virkkula et al (2007). This relies on BC concentration being the same between advances of the sample filter tape.
- AE31 – The AE31 is designed for wearable operation for part of a day under battery power. The deployment of the AE31 at Ealing 12 required several changes to the normal operation of this instrument. Firstly the instrument was connected to a mains power supply. Visits were made at one to four days intervals to change sample filters. As a consequence of this long

sample period the loading of each filter was much greater than when operated for personal sampling. The Virkulla et al (2007) approach was adapted to apply a single correction factor (k) across all samples in the way suggested by Park et al (2010). This single k factor was obtained from analysis of the North Kensington dataset.

- A measurement uncertainty of around 15% was estimated based on that for the UK black smoke network (Butterfield et al 2013).

Wind speed and wind direction were measured at London Heathrow.

## 5 Results

### 5.1 Gas and particle concentrations

Measured concentrations from the Ealing 12 monitoring site are shown in Table 1 along with urban background measurements for all pollutants for the 2012 calendar year. Very good data capture was achieved for NO<sub>x</sub>/NO<sub>2</sub> and PM<sub>10</sub> which operated for the whole year, with all measurands achieving the 90% data capture required in the EU air quality directive (2008/50/EC). Lower data capture was recorded for BC and CO<sub>2</sub> which were operated for part of the year only. Ealing 12 experienced greater concentrations than those measured at background for all pollutants except NO<sub>2</sub>. In contrast to expectations from modelled data the annual mean concentration at Ealing 12 was less than the AQS objective and EU Limit Value concentration of 40 µg m<sup>-3</sup> and no increment in NO<sub>2</sub> was found over that measured at Ealing 7. This similarity in NO<sub>2</sub> concentrations is also reflected in the 5<sup>th</sup>, 95<sup>th</sup> and median concentrations at the two sites. The maximum hourly mean NO<sub>2</sub> concentration at Ealing 12 was 178 µg m<sup>-3</sup>, less than the threshold for the short term EU Limit Value concentration for NO<sub>2</sub> (200 µg m<sup>-3</sup>).

	NO <sub>x</sub> µg m <sup>-3</sup>		NO <sub>2</sub> µg m <sup>-3</sup>		PM <sub>10</sub> µg m <sup>-3</sup>		BC µg m <sup>-3</sup>		CO <sub>2</sub> ppm	
Mean	88	54	35	35	23	21	2.4	1.6	409	401
5th %ile	11	10	8	9	9	8	0.3	0.3	385	378
Median	63	33	32	30	19	18	1.7	1.2	405	398
95th %ile	248	168	73	75	50	47	7.0	4.6	450	438
Capture	93%	91%	93%	91%	97%	98%	15%	15%	53%	46%

**Table 1 Ealing 12 measured concentrations (white) and those measured in the urban background (grey shading) for 2012. Data capture for BC is on matched days.**

Measured concentrations from the Islington 6 monitoring site are shown in Table 2 along with urban background measurements for all pollutants for 12 month period starting 26<sup>th</sup> July 2012. This period was selected in order to compare the Islington 6 site with the Tower Hamlets 5 background monitoring site which was installed part way through 2012. Again good data capture was achieved for NO<sub>x</sub>/NO<sub>2</sub> and PM<sub>10</sub> which operated for the whole year with lower data capture for BC and CO<sub>2</sub> which were operated for part of the year only. Islington 6 experienced greater concentrations than those

measured at background for all pollutants. In contrast to expectations from modelled data the annual mean concentration at Islington 6 was less than the AQS objective and EU Limit Value concentration of  $40 \mu\text{g m}^{-3}$ . The maximum hourly mean  $\text{NO}_2$  concentration at Islington 6 was  $265 \mu\text{g m}^{-3}$ . In total the monitoring site measured ten hours with mean concentrations above the EU short term limit value concentration of  $200 \mu\text{g m}^{-3}$ , on the 12<sup>th</sup> December 2012 and on 10<sup>th</sup>, 17<sup>th</sup> and 20<sup>th</sup> January 2013. The EU directive stipulates that not more than 17 such events should occur in any one year. The days with hourly mean  $\text{NO}_2$  above  $200 \mu\text{g m}^{-3}$  were not isolated to Islington 6. These were periods of poor pollutant dispersion when many London sites also experienced pollutant similar concentrations.

	$\text{NO}_x \mu\text{g m}^{-3}$		$\text{NO}_2 \mu\text{g m}^{-3}$		$\text{PM}_{10} \mu\text{g m}^{-3}$		$\text{BC} \mu\text{g m}^{-3}$		$\text{CO}_2 \text{ ppm}$	
Mean	58	48	39	33	23	21	2.4	2.0	418	414
5th %ile	16	10	13	9	8	7	0.5	0.3	393	394
Median	42	31	33	27	20	18	1.7	1.4	411	408
95th %ile	159	145	80	74	49	44	7.2	5.9	465	459
Capture	93%	96%	93%	96%	98%	97%	17%	17%	70%	67%

**Table 2 Islington 6 measured concentrations (white) and those measured in the urban background (grey shading) for the 12-months beginning 26<sup>th</sup> July 2012. Data capture for BC is on matched days.**

Differences between the Ealing 12 and Islington 6 monitoring sites can be seen by considering enrichment ratios. Enrichment ratios have been calculated using pollutant increments at each site above background for each pollutant, relative to the increment in  $\text{CO}_2$  as an indicator of local fuel combustion. Due to different measurement periods for each pollutant this calculation was undertaken for the period of the BC measurements only and is shown in Table 3. Comparing the two sites it is clear that local emissions of  $\text{NO}_x$ , per unit  $\text{CO}_2$ , at Ealing were around 1.7 times than those measured at Islington; BC was 1.4 times greater and  $\text{PM}_{10}$  was three times greater. By contrast  $\text{NO}_2$  per unit  $\text{CO}_2$  at was far greater at Islington when compared with Ealing, by a factor of five.

	$\text{NO}_x/\text{CO}_2$ ppb/ppm	$\text{NO}_2/\text{CO}_2$ ppb/ppm	$\text{PM}_{10}/\text{CO}_2$ $\mu\text{g m}^{-3}/\text{ppm}$	$\text{BC}/\text{CO}_2$ $\mu\text{g m}^{-3}/\text{ppm}$
Ealing 12	6.11	0.21	0.18	0.17
Islington 6	3.54	1.04	0.06	0.12

**Table 3 Local enrichment ratios, relative to  $\text{CO}_2$ , at Ealing 12 and Islington 6 for the period when BC measurements took place.**

Table 4 shows  $\text{NO}_2$  diffusion tube measurements for 2012. These clearly indicate concentrations below the EU Limit Value of  $40 \mu\text{g m}^{-3}$  adjacent to the railway line. With a prevalent south-westerly wind, diffusion tubes on the north side of the Paddington Mainline would be expected to measure greater concentrations than their counterparts on the south side. Although this was the case for two of the three pairings, the cross track differences ( $1$  and  $2 \mu\text{g m}^{-3}$ ) were very small. At West Ealing the north tube measured less than the south one, however this part of the line has a complicated layout with sidings and junctions. At Islington both sites measured concentrations below the EU Limit Value.

Location	NO <sub>2</sub> µg m <sup>-3</sup>
Ealing -Southall, north of tracks (23)	39
Ealing - Southall, south of tracks (22)	37
Ealing – West Ealing, north of tracks (6)	34
Ealing - West Ealing south of tracks (7)	37
Ealing - Acton, north of tracks (97)	39
Ealing - Acton, south of tracks (98)	38
Islington – west (AG1)	37
Islington – east (AG2)	38

Table 4 NO<sub>2</sub> diffusion tube measurements 2012.

## 5.2 PM composition.

Mean concentrations of BC and metals are shown in Figure 7 for the Ealing and Islington railways site. Measurements at the North Kensington background site and Marylebone Road are shown for the same days as measurements at Ealing. Concentrations of BC were greater than that of the combined metals concentrations at all of the sites. Metals concentrations were dominated Fe, Ca Na and Ba at each site. It is clear from Figure 7 that both railway sites experienced concentrations above those at background indicating the presence of local sources. The railway also sites experienced similar concentrations of BC and metals, despite the different measurement periods.

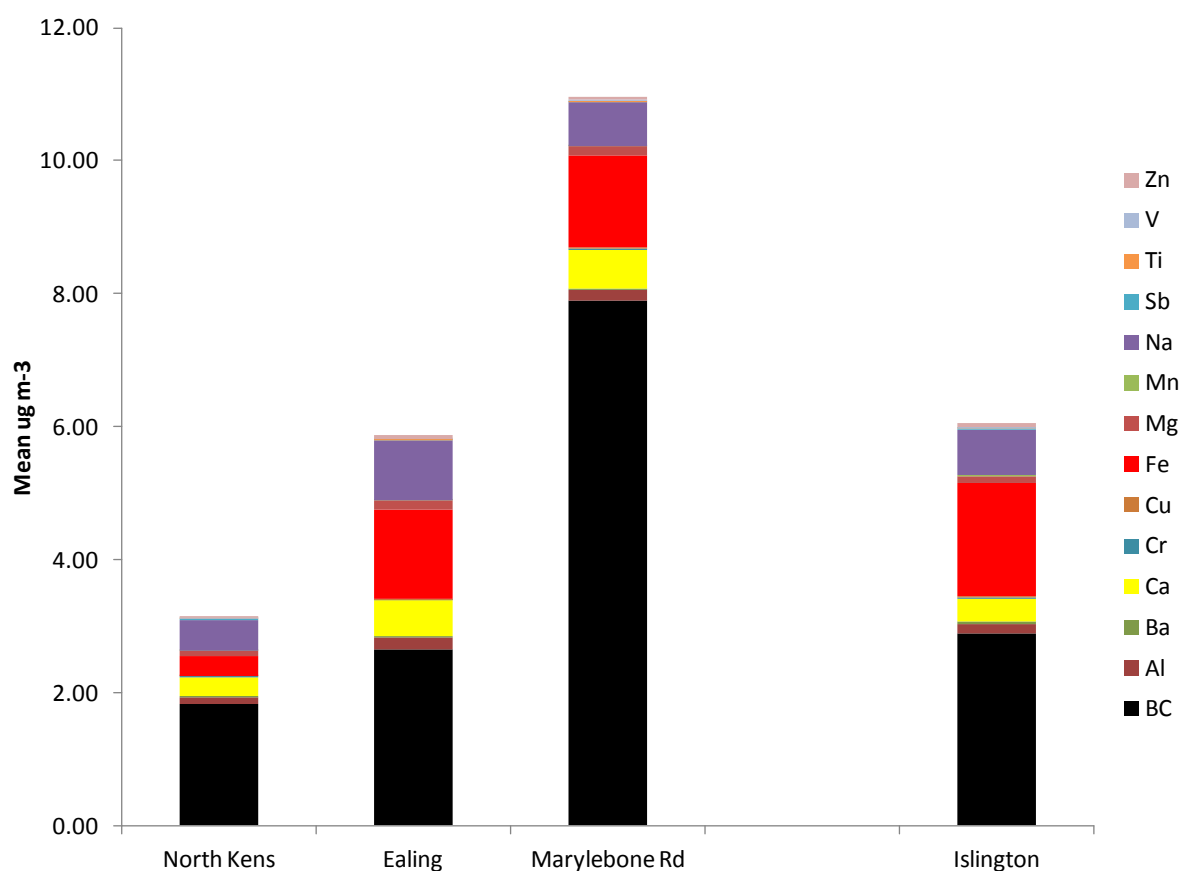


Figure 7 Mean concentrations of BC and metals.



## 6 Analysis of PM composition and local sources

Insights into the sources of metal particulate can be gained by considering correlations between each PM component. Table 5 shows the correlations at North Kensington. Two main sources can be seen within this data. Firstly a sea salt source can be seen in the good correlation between Na and Mg; the two most abundant anions in sea water. Greatest concentrations of sea salt PM occur during high wind speeds from the Atlantic. The negative correlations between Na and all other metals and BC suggests that these are occurring at different times; with BC and metals being greater during times of weaker dispersion for example or during times of continental air masses (Jones and Harrison, 2006). The remaining high positive correlations are largely reflective of non-exhaust emissions from traffic; especially brake wear with Cu and Fe from discs along with Ba and Sb from brake pads. The association of these sources with vehicle activity is underlined by the correlations with BC traffic exhaust emissions. Correlations between Fe and Mn in turn reflect the composition of steel in braking systems. (Thorpe and Harrison, 2008). The correlation between Cr and V reflects analytical difficulties in separating these metals.

	BC	Al	Ba	Ca	Cr	Cu	Fe	Mg	Mn	Na	Sb	Ti	V	Zn
BC	1.00													
Al	0.48	1.00												
Ba	0.85	0.68	1.00											
Ca	0.52	0.80	0.72	1.00										
Cr	0.44	0.29	0.38	0.39	1.00									
Cu	0.79	0.71	0.90	0.74	0.44	1.00								
Fe	0.84	0.77	0.95	0.79	0.47	0.93	1.00							
Mg	-0.28	0.14	-0.14	0.33	0.03	-0.14	-0.05	1.00						
Mn	0.74	0.74	0.80	0.89	0.45	0.81	0.88	0.18	1.00					
Na	-0.44	-0.26	-0.43	-0.04	-0.03	-0.46	-0.37	0.89	-0.13	1.00				
Sb	0.93	0.59	0.91	0.61	0.46	0.90	0.92	-0.24	0.78	-0.49	1.00			
Ti	0.57	0.93	0.77	0.87	0.25	0.73	0.80	0.19	0.83	-0.19	0.65	1.00		
V	0.50	0.34	0.42	0.43	0.99	0.46	0.50	0.03	0.50	-0.04	0.49	0.30	1.00	
Zn	0.55	0.44	0.55	0.48	0.64	0.71	0.63	0.06	0.60	-0.13	0.63	0.39	0.65	1.00

Table 5 Correlation coefficients ( $r$ ) between BC and PM metals at North Kensington. Coefficients above 0.85 are highlighted.

Correlation coefficients at Ealing are shown in Table 6. Sources here are similar to North Kensington with sea salt (Na, Mg), and brake wear (Cu, Fe, Sb, Ba) all clearly present along with Fe and Mn reflecting steel wear. The associations between these sources and BC is however weaker suggesting that different processes might be affecting exhaust and these other sources of metals.

	BC	Al	Ba	Ca	Cr	Cu	Fe	Mg	Mn	Na	Sb	Ti	V	Zn
BC	1.00													
Al	0.46	1.00												
Ba	0.77	0.58	1.00											
Ca	0.56	0.81	0.72	1.00										
Cr	-0.16	-0.16	-0.23	-0.40	1.00									
Cu	0.79	0.45	0.96	0.65	-0.29	1.00								
Fe	0.80	0.73	0.94	0.80	-0.22	0.89	1.00							
Mg	-0.34	0.02	-0.28	0.05	-0.12	-0.28	-0.23	1.00						
Mn	0.81	0.77	0.87	0.83	-0.27	0.82	0.95	-0.12	1.00					
Na	-0.43	-0.40	-0.48	-0.30	-0.15	-0.41	-0.51	0.87	-0.43	1.00				
Sb	0.76	0.48	0.94	0.63	-0.29	0.94	0.87	-0.44	0.80	-0.56	1.00			
Ti	0.56	0.97	0.70	0.85	-0.17	0.57	0.83	-0.02	0.85	-0.42	0.59	1.00		
V	0.01	-0.07	-0.13	-0.30	0.97	-0.17	-0.11	-0.15	-0.14	-0.20	-0.20	-0.07	1.00	
Zn	0.65	0.50	0.71	0.55	-0.32	0.73	0.72	-0.39	0.73	-0.53	0.84	0.57	-0.21	1.00

Table 6 Correlation coefficients ( $r$ ) between BC and PM metals at Ealing. Coefficients above 0.85 are highlighted.

Correlation coefficients at Islington are shown in Table 7. In addition to brake wear (Cu, Ba, Sb), iron (Fe, Mn) and sea salt (Na, Mg) sources, additional high correlations can be seen between Zn and the brake wear components, Ba and Sb and also with Mn. Zn is the most abundant metal in tyre wear particles and often used as a tracer for this source suggesting the presence of both brake and tyre wear sources near the site. Ca and Al are often indicators of mineral sources or road wear along with Ti (Thorpe and Harrison, 2008).

	BC	Al	Ba	Ca	Cr	Cu	Fe	Mg	Mn	Na	Sb	Ti	V	Zn
BC	1.00													
Al	-0.09	1.00												
Ba	0.66	0.03	1.00											
Ca	0.08	0.96	0.21	1.00										
Cr	0.35	-0.01	0.47	0.10	1.00									
Cu	0.55	0.01	0.97	0.17	0.48	1.00								
Fe	0.58	0.27	0.88	0.42	0.44	0.85	1.00							
Mg	-0.23	0.73	0.12	0.77	0.02	0.16	0.35	1.00						
Mn	0.65	0.37	0.71	0.51	0.46	0.67	0.86	0.39	1.00					
Na	-0.24	0.55	0.11	0.61	0.01	0.17	0.32	0.96	0.34	1.00				
Sb	0.85	-0.06	0.79	0.10	0.35	0.71	0.73	-0.06	0.77	-0.08	1.00			
Ti	0.12	0.91	0.40	0.93	0.12	0.37	0.54	0.72	0.56	0.56	0.24	1.00		
V	0.48	0.08	0.38	0.18	0.89	0.38	0.39	-0.01	0.54	-0.04	0.40	0.17	1.00	
Zn	0.78	0.17	0.87	0.34	0.47	0.83	0.79	0.15	0.86	0.11	0.87	0.47	0.57	1.00

Table 7 Correlation coefficients ( $r$ ) between BC and PM metals at Islington. Coefficients above 0.85 are highlighted.

Greater focus on the local sources affecting a monitoring site can be obtained through considering the increment in concentrations above the background. This is possible for the Ealing site where contemporaneous measurements are available from North Kensington as shown in Table 8. Here the local nature of brake wear (Cu, Ba, Sb) and a separate steel (Fe, Mn) source can be clearly seen. The separation of these two sources suggests that the Fe and Mn source might be related to two sources; traffic and track wear for instance.

	eBC	Al	Ba	Ca	Cr	Cu	Fe	Mg	Mn	Na	Sb	Ti	V	Zn
eBC	1.00													
Al	0.23	1.00												
Ba	0.67	0.44	1.00											
Ca	0.35	0.66	0.53	1.00										
Cr	-0.15	-0.25	-0.24	-0.38	1.00									
Cu	0.64	0.25	0.87	0.42	-0.28	1.00								
Fe	0.62	0.76	0.74	0.67	-0.25	0.67	1.00							
Mg	-0.15	-0.08	-0.12	-0.06	-0.02	-0.22	-0.14	1.00						
Mn	0.64	0.76	0.76	0.69	-0.21	0.64	0.94	-0.19	1.00					
Na	-0.16	-0.51	-0.24	-0.36	-0.13	-0.19	-0.44	0.82	-0.51	1.00				
Sb	0.59	0.37	0.89	0.49	-0.24	0.89	0.73	-0.36	0.72	-0.40	1.00			
Ti	0.38	0.87	0.60	0.73	-0.27	0.33	0.77	-0.10	0.81	-0.49	0.48	1.00		
V	-0.04	-0.20	-0.19	-0.32	0.99	-0.22	-0.17	-0.05	-0.13	-0.17	-0.20	-0.22	1.00	
Zn	0.32	0.39	0.58	0.42	-0.21	0.68	0.56	-0.47	0.59	-0.52	0.75	0.38	-0.15	1.00

**Table 8** Correlation coefficients ( $r$ ) between BC and PM metals in the concentration increment between Ealing and North Kensington. Coefficients above 0.85 are highlighted.

Analysis of concentrations by wind direction can often provide information about source location. As pointed out by Cosemans et al (2008) specific approaches are required to produce accurate pollution roses with daily measured concentrations. These combine the daily measured metal concentrations with highly resolved meteorological data. Figure 8 shows mean metals concentration by wind direction at Ealing. Similar source locations were seen for possible track and electric conductor wear tracers (Fe, Cu, Mn) with sources being greatest between 60° and 280° consistent with the location of the railway. However this distribution is also similar to that of Zn, a tracer for tyre wear and Ba as a tracer for vehicle brake wear suggesting that traffic sources are making a very substantial contribution to the Fe, Cu and Mn at the site. This contrasts with that of Na being mainly from sea salt.

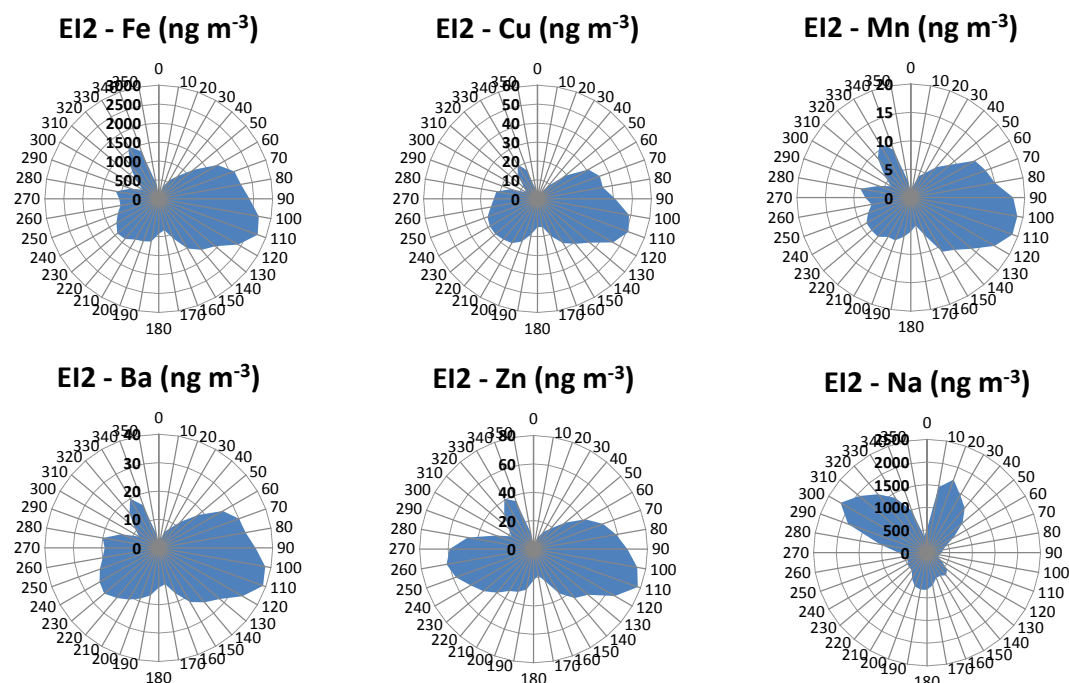


**Figure 8** Mean metal concentrations by wind direction at Ealing.

Analysis of the concentration increment between Ealing and North Kensington (Figure 9) shows some separation between steel (Fe, Mn) and Cu wear (brakes, conductor and track wear) and the wind

dependency for Ba (brake wear) and Zn (tyre wear) however it is not possible to clearly differentiate between these sources. The presence of a local Na source suggests a contribution from road salting on the residential streets to the north of the monitoring sites.

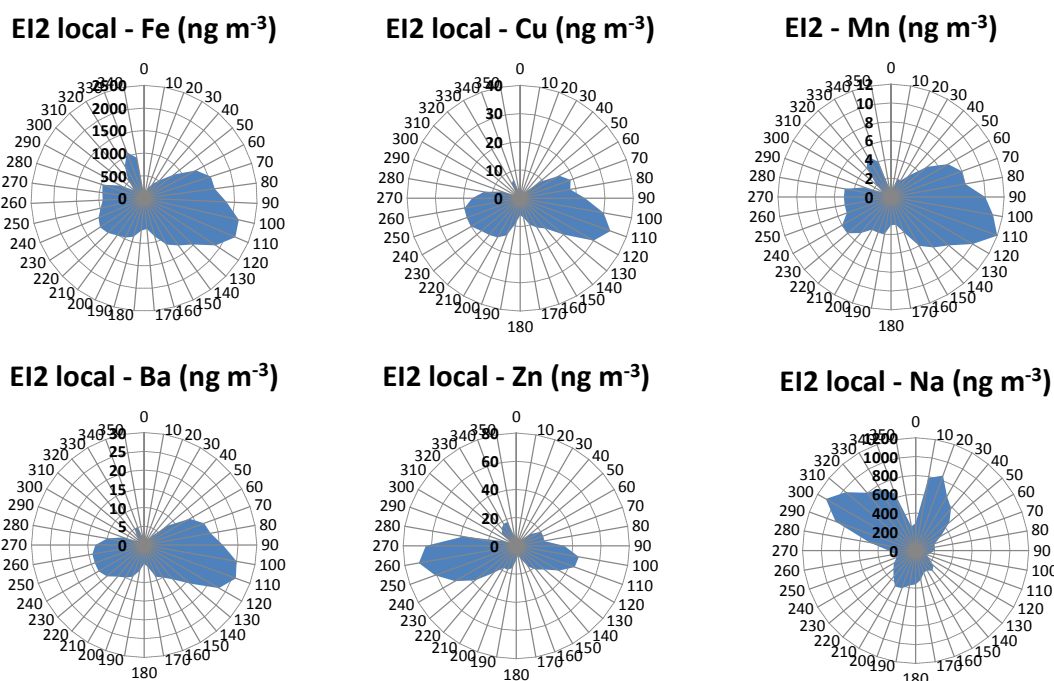


*Figure 9 Mean metal concentrations by wind direction in the concentration increment between Ealing and North Kensington.*

The mean concentration of metals at Islington (Figure 10) shows no clear separation between tracers for track wear (Fe, Mn), conductor wear (Cu), brake wear (Cu, Fe, Ba) and traffic tyre wear (Zn). A clear south-west influence can be seen in Na consistent with a sea salt source.

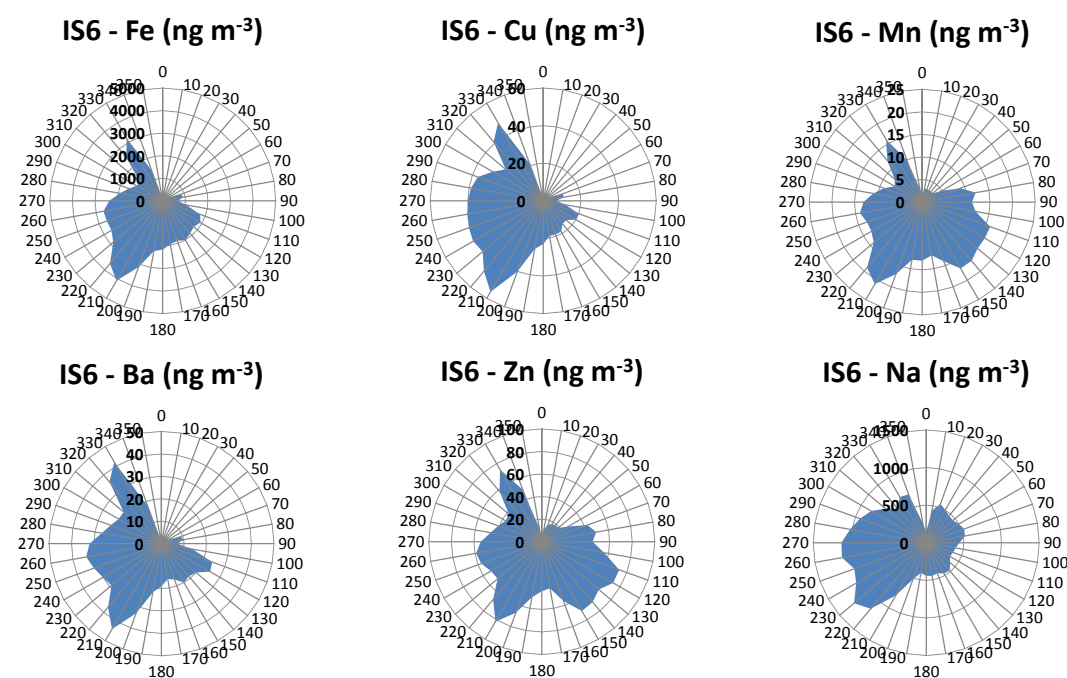


Figure 10 Mean metal concentrations by wind direction at Islington.

In summary there is only weak evidence that metals measured at the monitoring sites might be due to a railway source in addition to that from non-exhaust emission from road traffic. This evidence is strongest in the concentration increment at Ealing. However it is apparent from Figure 7 that the concentrations of Fe at both Islington and Ealing are greater than what might be expected on the basis of the black carbon as an indicator for diesel vehicle activity.

As an alternative approach we sought to estimate the Fe from track wear using a relationship between BC and Fe for traffic sources from the concentration increment between the Marylebone Road monitoring site and North Kensington. Reduced or standardised major axis regression was used. This yielded the relationship:

$$[\text{Fe}] = 0.12 \pm 0.02[\text{BC}] + 0.39 \pm 0.20, r = 0.69$$

where uncertainties are expressed at  $2\sigma$ .

Applying this equation to the increment in BC concentrations at Ealing yields and estimated mean Fe concentration of  $0.8 \pm 0.5 \mu\text{g m}^{-3}$  assuming all local BC and Fe was arising from traffic. Comparing this estimate to the measured mean of  $1.3 \pm 0.2 \mu\text{g m}^{-3}$  suggests that additional mean concentration of  $0.5 \pm 0.3 \mu\text{g m}^{-3}$  Fe was present at Ealing; representing some  $40 \pm 20 \%$  of Fe at Ealing. This would be  $0.8 \pm 0.5 \mu\text{g m}^{-3}$  as a contribution to  $\text{PM}_{10}$ , if all Fe was present as  $\text{Fe}_2\text{O}_3$ .

A similar calculation for Islington, assuming background conditions at North Kensington during early 2012 apply to the this period yields an additional mean concentration for Fe of  $0.9 \pm 0.6 \mu\text{g m}^{-3}$  or around  $50 \pm 30\%$ . This would be  $1.2 \pm 0.8 \mu\text{g m}^{-3}$  as a contribution to  $\text{PM}_{10}$ , if all Fe was present as  $\text{Fe}_2\text{O}_3$ .

A similar approach can be taken with using Ba as a tracer to predict the Fe at each site expected from traffic and assume that any excess Fe is due to track wear. The standardised major axis regression

from concentration increment between the Marylebone Road monitoring site and North Kensington yielded the relationship:

$$[\text{Fe}] = 36 \pm 4[\text{Ba}] + 0.49 \pm 0.08, r = 0.71$$

Using this approach the additional Fe at Ealing was predicted to be  $0.15 \pm 0.08 \mu\text{g m}^{-3}$  ( $0.21 \pm 0.11 \mu\text{g m}^{-3}$  as  $\text{Fe}_2\text{O}_3$ ) and the additional Fe at Islington was predicted to be  $0.13 \pm 0.06 \mu\text{g m}^{-3}$  as Fe ( $0.18 \pm 0.09 \mu\text{g m}^{-3}$  as  $\text{Fe}_2\text{O}_3$ ).

Here uncertainties have been estimated based on the methods in ISO GUM ((BIPM et al 2008) and expressed using a coverage factor of  $k=2$  which approximates to  $2\sigma$ .

## 7 Analysis of $\text{NO}_x$ , $\text{NO}_2$ and $\text{PM}_{10}$ concentrations along with $\text{CO}_2$

### 7.1 Preliminary considerations

It is useful to get a feel for the concentrations at the Ealing 12 monitoring site. The site is around 10 m from the rail track edge with no other sources between the site and the rail track itself. A background site (Ealing 7) is located about 600 m away from the site and is ideally located for use in subtracting concentrations from the Ealing 12 site.

Based on  $\text{NO}_x$  data from April 2011 to December 2013, the increment in  $\text{NO}_x$  above the background site is about  $36 \mu\text{g m}^{-3}$ . This increment can be considered to be relatively small given the proximity of the railway. It should also be stressed that one of the motivations for this work was that model predictions showed the railway at this location to be a very important source of  $\text{NO}_x$  and  $\text{NO}_2$ . It is clear from the increment in  $\text{NO}_x$  discussed above that the measurement evidence for a dominant and important source of  $\text{NO}_x$  does not support this view – even without finessing the analysis further.

A consideration of the  $\text{NO}_x$  polar plot (Figure 11) shows that the increment in  $\text{NO}_x$  concentrations at this site is indeed dominated by sources to the south i.e. sources in the direction of the railway. However, there is more evidence of higher concentrations from the east/south-east. This feature is from the direction of Southall station, which might indicate a rail source for trains at the station itself. However, as shown in Figure 11, the A3005 crosses the railway also in the same direction. It cannot be concluded from this plot alone that the pattern of concentration seen in Figure 11 is definitively a rail or road source. However, it is known from the analysis of other road sources (because most monitoring sites are located close to roads rather than railways) that the pattern of concentration seen in Figure 11 could be a road of that type. A key question therefore is whether there is other evidence that would point to the source being dominated by road vehicle emissions or diesel train emissions.

s





*Figure 11 Bivariate polar plot of  $\text{NO}_x$  concentrations at the Ealing 12 railway site. Background concentrations have been subtracted using the nearby Ealing 7 site.*

In addition to the analysis above the concentrations at the background Ealing 7 site (about 600 m north of the railway) can be considered. There are no road sources between the Ealing 7 site and the railway. If rail sources were very important (as indicated by dispersion modelling) then it might be expected that they would be detected at Ealing 7. However a consideration of polar plots from the Ealing 7 site show there is no apparent signal due to a rail source. The plot for  $\text{NO}_2$  is revealing however and shows the contribution from London in general to the east and (most likely) Heathrow Airport to the south-west. This is consistent with Carslaw et al (2006) who found that  $\text{NO}_2$  from Heathrow could be detected at monitoring sites some 3 km from the airport. The polar plot is shown in Figure 12.

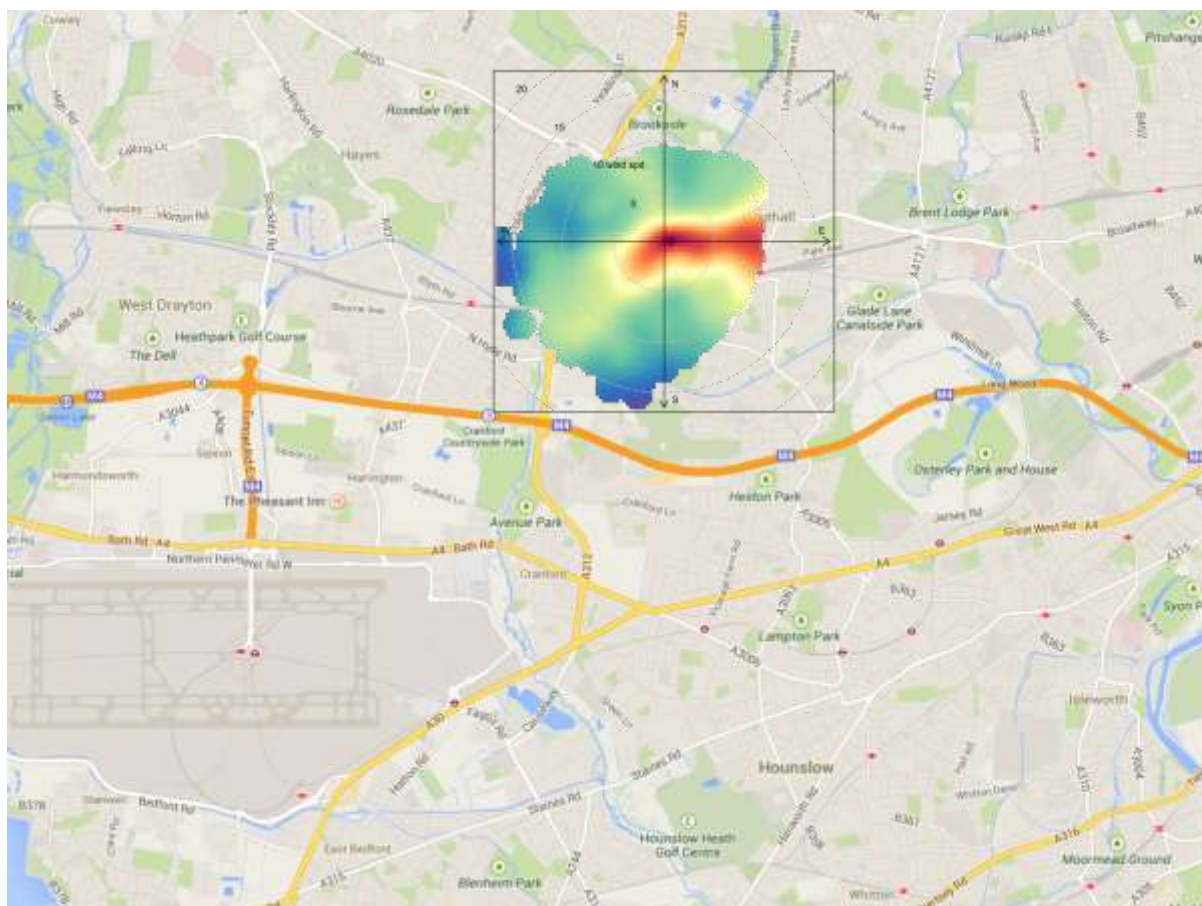


Figure 12 Bivariate polar plot of NO<sub>2</sub> concentrations at the Ealing 7 background site.

## 7.2 Emissions considerations

It is useful to compare the emissions assumed in the LAEI for the rail lines passing the measurement site with other sources to develop an understanding of whether it is reasonable to detect a rail source. Data from the LAEI 2010 suggest that the total emissions of NO<sub>x</sub> for the railway (passenger and freight) are about 62 t/km/yr. This figure can usefully be compared with the M25, which on average is 46 t/km/yr or Marylebone Road (38 t/km/yr). The estimated rail emissions of NO<sub>x</sub> at the Ealing site are therefore high and this is the reason that modelled concentrations are also high. The comparison with Marylebone Road is particularly useful because the ambient measurements are high for NO<sub>x</sub> and NO<sub>2</sub> and clearly reflect the very dominant local source of the road. The rail source of NO<sub>x</sub> is 25% more than Marylebone Road and should be easily detectable where the site is located.

The ratio of NO<sub>x</sub>/CO<sub>2</sub> given in the inventory is entirely reasonable given what is known about emissions from large diesel engines. The total emissions are high because of the high activity of diesel trains at this location. Assuming the rail activity data are correct then it does seem reasonable that the rail source would have a significant impact on near-field NO<sub>x</sub> and NO<sub>2</sub> concentrations.

The LAEI also provides estimates of CO<sub>2</sub> emissions that allows ratios of NO<sub>x</sub>/CO<sub>2</sub> to be calculated. On average the rail source NO<sub>x</sub>/CO<sub>2</sub> ratio is 0.013, which is consistent with expectations based on emissions from large diesel engines. The analysis of NO<sub>x</sub> and CO<sub>2</sub> concentrations shows that there is no obvious train source signature. The ratio of NO<sub>x</sub>/CO<sub>2</sub> is helpful in comparing similar estimates from

the ambient data. For example, it would not be expected that the ratio of  $\text{NO}_x/\text{CO}_2$  from a dominant diesel emission source would be less than  $\sim 0.01$ ; unless there was some form of aftertreatment (such as Selective Catalytic Reduction) used. Ratios well below 0.01 would more likely be associated with other sources and would not be consistent with diesel trains without  $\text{NO}_x$  emissions control.

### 7.3 Linking with measured pollutants including $\text{CO}_2$

#### *The Bentley approach*

The aim of this section is to determine whether a source contribution from the railway can be detected, understood and quantified. Measurements of  $\text{NO}_x$  and  $\text{CO}_2$  together should help better understand the contribution of  $\text{NO}_x$  from combustion sources. Specifically, if plumes of  $\text{NO}_x$  and  $\text{CO}_2$  can be detected then it should be possible to quantify a  $\text{NO}_x/\text{CO}_2$  ratio, which can then be related to fuel use. In particular a  $\text{NO}_x/\text{CO}_2$  ratio can be compared directly with emission inventory estimates to determine their accuracy and also be used as the basis of correcting emission inventories.

The relationship between the increment in  $\text{NO}_x$  and  $\text{CO}_2$  at Ealing 12 above background Ealing 7 is not very clear from a scatter plot (Figure 13) suggesting that the data are perhaps too noisy to discern any clear relationship.

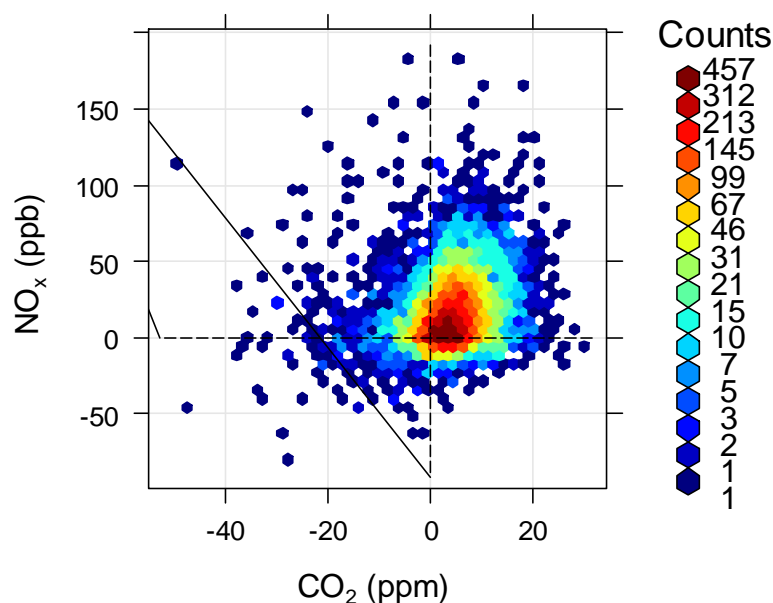


Figure 13 Scatter plot of the increment in  $\text{CO}_2$  vs. the increment in  $\text{NO}_x$  at the EI2 site. Data have been binned to help reveal where most of the points lie.

Given the noisy nature of the data, an innovative approach was used to understand whether  $\text{NO}_x/\text{CO}_2$  ratios could be estimated. The idea is based on Bentley (2004) and it works as follows. The data are split up into consecutive sequences of three hour periods. For each group of three points a regression is carried out relating  $\text{NO}_x$  and  $\text{CO}_2$  concentrations. If there is a good relationship ( $R^2 > 0.95$ ) the group

is retained if not it is not used. For typical data sets this process results in a series of regression lines linking  $\text{NO}_x$  and  $\text{CO}_2$ . From the regressions the slope of the  $\text{NO}_x$ - $\text{CO}_2$  fits are recorded. The basic idea is that as local plumes are diluted through dispersion *all species are diluted by the same amount*. By considering many groups, patterns can be revealed that show consistent ratios between the pollutants.

To illustrate the technique  $\text{NO}_x$  and  $\text{CO}_2$  have been considered for hourly data in 2012 for Marylebone Road. Figure 14 shows that these 'dilution lines' tend to run parallel to one another which is indicative of a plume being diluted by atmospheric mixing and/or due to changes in local source strengths. Note that only 200 lines are shown for clarity.

For many situations working with absolute data rather than trying to remove a background concentration can be a good idea. This is because the results could depend strongly on the appropriate choice of a background site, which can be difficult to judge. An advantage of the Bentley technique therefore is that no background concentration is required.

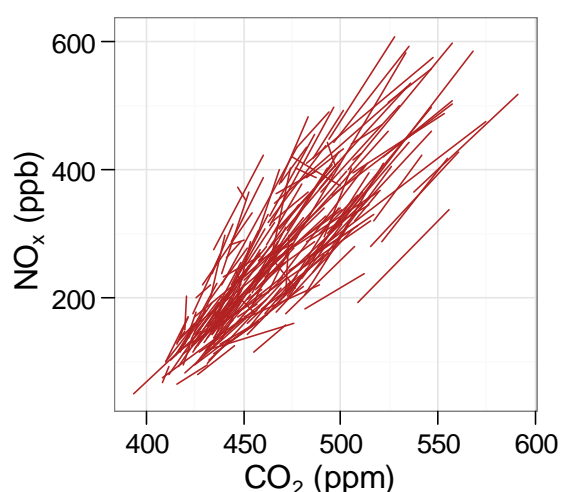


Figure 14 Run-regression lines relating concentrations of  $\text{CO}_2$  and  $\text{NO}_x$  at Marylebone Road. The analysis is based on consecutive 3-hour means.

The gradients of the dilution lines shown above can be analysed to determine the most frequent occurrence. A histogram is shown in Figure 15 for the gradients of the dilution lines. This shows a peak at 3.5 ppb/ppm (or 0.0035 if the same units such as ppb are used). This is the best estimate of the relationship between  $\text{NO}_x$  and  $\text{CO}_2$ . Note however that a spread in values would be expected because emissions themselves will vary each hour and it would not be expected the ambient  $\text{NO}_x/\text{CO}_2$  ratio would remain absolutely constant.

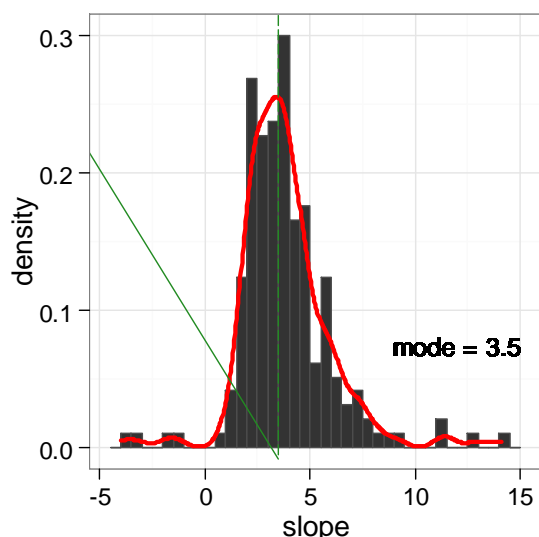


Figure 15 Histograms of run-regression line slopes for the  $\text{NO}_x/\text{CO}_2$  ratio at Marylebone Road.

## Ealing 12

The results shown above for Marylebone Road are very clear and other simpler techniques would probably be as effective. However, the situation at Ealing is not as straightforward and the Bentley technique may offer additional advantages over other approaches. The other aspect of the Marylebone Road results is that they provide a good example of how a large and clear local source can be when analysed in this way.

Figure 16 shows the dilution lines for the Ealing 12 site, where there is some indication of a consistent pattern – but not to the same extent as Figure 14. Compared to the results for Marylebone Road (Figure 14), the lines are much less clear. These results actually reveal a lot about the type of source close to Ealing. If for example train sources were very important to local  $\text{NO}_x$  and  $\text{CO}_2$  concentrations then it would be expected the pattern of regression lines would be much clearer – and the concentrations higher than they are. This is not the case, which strongly suggests that the rail source (or other sources) does not have a large influence on concentrations at this particular location. Furthermore, a strong rail source would also be expected to have a very clear relationship between  $\text{NO}_x$  and  $\text{CO}_2$  because the source is 100% diesel in origin. This contrasts with road vehicle sources where a significant fraction of the emissions is due to petrol vehicles (an important source of  $\text{CO}_2$  but a minor source of  $\text{NO}_x$ ).

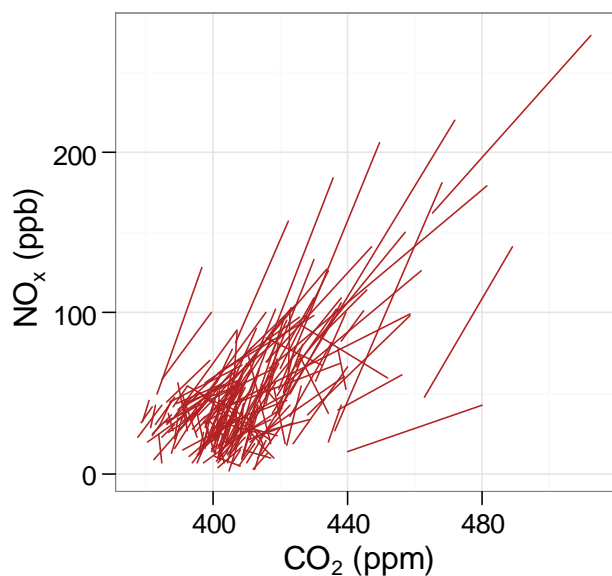


Figure 16 Example of 200 run-regression lines relating concentrations of  $\text{CO}_2$  and  $\text{NO}_x$  at the Ealing 12 site. The analysis is based on consecutive hourly means with the background concentrations removed using the Ealing 7 site.

In the case of the Ealing 12 site the  $\text{NO}_x/\text{CO}_2$  ratio was calculated to be 2.5 ppb/ppm (0.0025 using the same units). This value is somewhat lower than at Marylebone Road. This might be expected if the source was dominated by road vehicles and there were fewer diesel vehicles in Ealing compared with Marylebone Road (which will be the case). If the Ealing 12 site were dominated by diesel trains it might be expected that the  $\text{NO}_x/\text{CO}_2$  ratio would be higher (around 0.01). These results suggest that the source seen to the south of the site is not dominated by diesel train emissions.

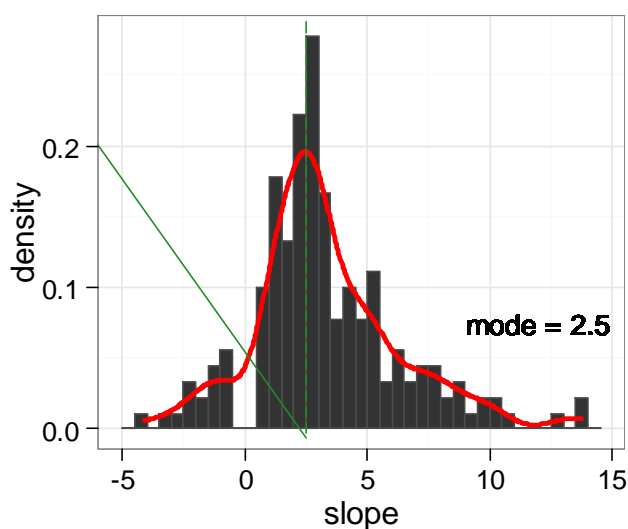


Figure 17 Histograms of run-regression line slopes for the  $\text{NO}_x/\text{CO}_2$  ratio at Ealing 12 without background concentrations removed.



No sensible results could be generated for black carbon because there were too few of them. However, results for  $\text{PM}_{10}/\text{NO}_x$  were calculated using data where no background concentrations were removed, shown in Figure 18. On average the mode for  $\text{PM}_{10}$  was around  $0.13 \text{ } (\mu\text{g m}^{-3}/\text{ppb})$ . Using  $\text{NO}_x$  on a mass basis as well the slope would be 0.06, which is in good agreement with ratios at roadside locations elsewhere in London and previous analysis by Fuller and Green (2006). For example the results for Marylebone are also shown in Figure 18 where the mode is slightly lower than Ealing 12 (0.11 vs. 0.13). On the other hand the EI2 results are more skewed towards higher concentrations than Marylebone Road. Indeed, if the median values are taken then Ealing 12 has a slope of 0.18 and Marylebone Road has a slope of 0.12. These results might provide some evidence of sources with an increased  $\text{PM}_{10}/\text{NO}_x$  ratio at the Ealing 12 site (such as diesel trains) but it is difficult to be certain. Furthermore, even if the emissions with a higher  $\text{NO}_x/\text{CO}_2$  ratio were trains, they would not seem to dominate at this location.

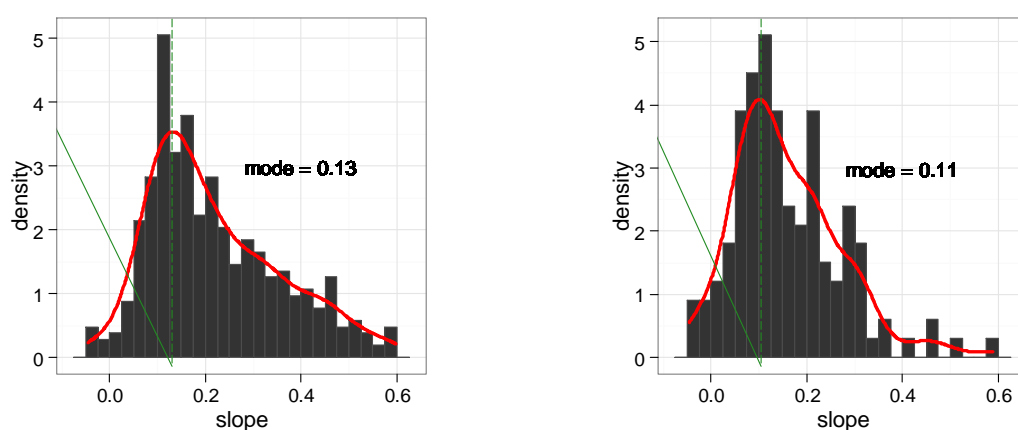


Figure 18 Histograms of run-regression line slopes for the  $\text{PM}_{10}/\text{NO}_x$  ratio at Ealing 12 (left) and Marylebone Road (right).

It is also useful to consider the temporal variation in concentrations of  $\text{NO}_x$ ,  $\text{CO}_2$  and  $\text{PM}_{10}$  to determine whether there are any clues to suggest whether the source is likely to be related to diesel trains or other sources such as road vehicles. Considering the diurnal plot shown in Figure 19 it is clear that there are two peaks during the day in both  $\text{NO}_x$  and  $\text{PM}_{10}$  – but the peak in  $\text{CO}_2$  is less clear in the morning. These plots confirm a combustion source to the south of the Ealing 12 monitoring site. The other plot to note is the day of the week plot that clearly shows concentrations of  $\text{NO}_x$  and  $\text{PM}_{10}$  are much lower at weekends and in particular on Sundays. This sort of variation is typical of road traffic sources where there are fewer heavy duty vehicles at the weekend. However, concentrations of  $\text{CO}_2$  were not lower at weekends, which makes the interpretation more difficult. On its own Figure 19 does not help identify whether the source is road transport or railway dominated.

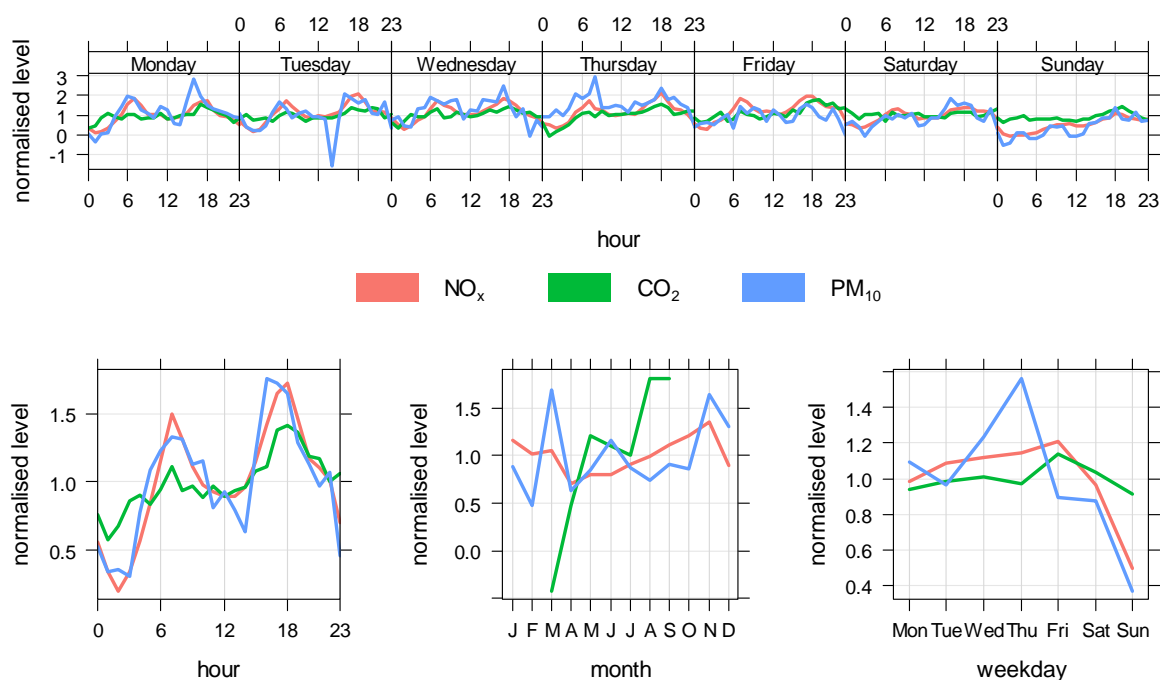


Figure 19 Temporal variation in  $\text{CO}_2$ ,  $\text{NO}_x$  and  $\text{PM}_{10}$  concentrations at Ealing 12 for wind directions from 90 to 270 degrees i.e. those from the railway. Note that the background concentrations have been removed and the concentrations normalised to allow a comparison between pollutants with very different concentration ranges.

Published emission factors for diesel trains e.g. Table 6 in Hobson and Smith (2011) (see here <http://www.dpea.scotland.gov.uk/Documents/qj13769/A1892587.PDF>) for 30 different diesel trains suggest a mean  $\text{NO}_x/\text{CO}_2$  ratio of 0.0094. A ratio of around 0.01 is very similar to that for large vehicles (HGVs and buses) based on the vehicle emission remote sensing analysis, suggesting that large diesel engines tend to emit very similar amounts of  $\text{NO}_x$  for a given amount of fuel burned (Carslaw and Rhys-Tyler, 2013). Lower  $\text{NO}_x/\text{CO}_2$  ratios for diesel engines might be expected if the exhaust is treated in some way e.g. through the use of Selective catalytic Reduction which would abate  $\text{NO}_x$  but not affect  $\text{CO}_2$ . However, diesel trains do not use such technology and there is no reason to believe the  $\text{NO}_x/\text{CO}_2$  ratios will differ much from 0.01.

### Islington

Again using the Bentley approach, consistent  $\text{NO}_x$ - $\text{CO}_2$  relationships can be extracted from the absolute concentration data, as shown in Figure 20. These relationships show the  $\text{NO}_x/\text{CO}_2$  ratio to be about 1.4 ppb / ppm or 0.0014 when expressed in same units, (Figure 21) which is a factor of two lower than the Ealing 12 site or Marylebone Road. Such low ratios would be consistent with non-diesel sources, or a mixed source such as road traffic where there was a relatively large influence due to light duty vehicles. In the case of Islington 6 there is no obvious  $\text{NO}_x/\text{CO}_2$  ratios that would appear to be consistent with a diesel train source i.e. a ratio of  $\text{NO}_x/\text{CO}_2$  around 0.01. From the analysis it would appear that there is no obvious indication of a train combustion source – or one that is significant enough to be clearly detected.

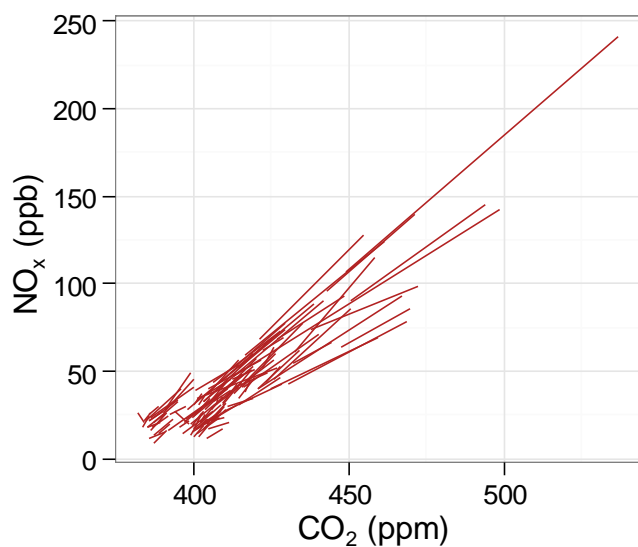


Figure 20 Run-regression lines relating concentrations of CO<sub>2</sub> and NO<sub>x</sub> at Islington 6. The analysis is based on consecutive 3-hour means.

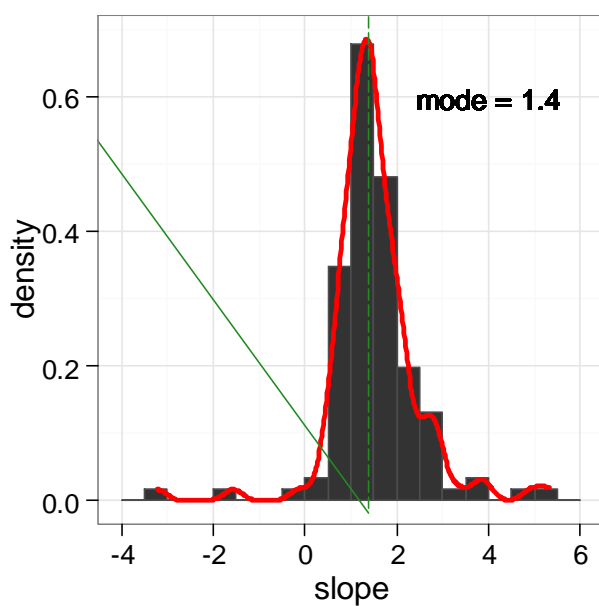


Figure 21 Histograms of run-regression line slopes for the NO<sub>x</sub>/CO<sub>2</sub> ratio at Islington 6 without background concentrations removed.

The polar plots for NO<sub>x</sub> at this location (Figure 22) suggested a source to the SSW, which would not be expected to be due to a railway source because of the direction. However, even excluding these directions from the analysis had little effect of the NO<sub>x</sub>/CO<sub>2</sub> ratios.

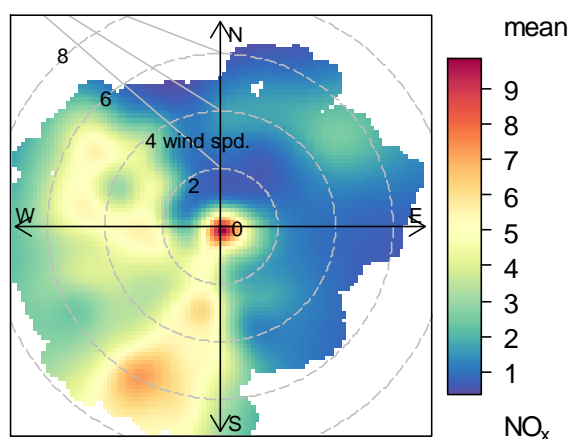


Figure 22 Polar plot of  $\text{NO}_x$  concentrations at Islington 6 with North Kensington background removed (2007-2013).

For  $\text{PM}_{10}/\text{NO}_x$  the estimated ratio is higher than was found at Ealing (0.22 vs. 0.13).

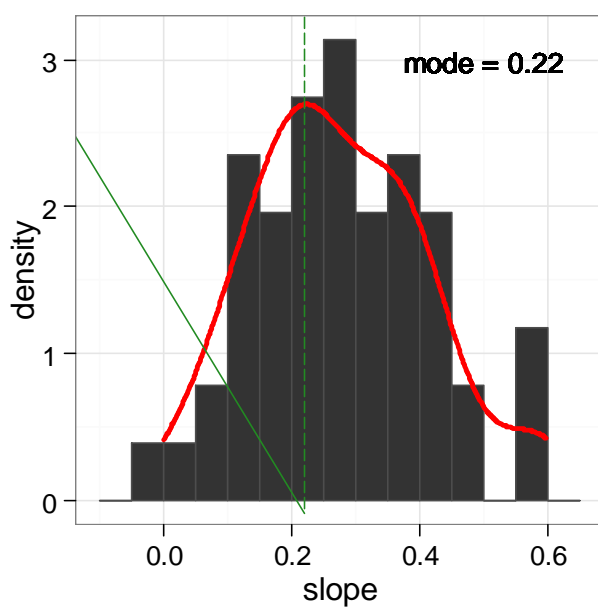


Figure 23 Histograms of run-regression line slopes for the  $\text{PM}_{10}/\text{CO}_2$  ratio at Islington 6 without background concentrations removed.

## 8 Emissions and dispersion modelling

### 8.1 Method

#### *Rail line selection*

Both Paddington and East Coast mainlines were selected from the national rail network covering London up to the M25 (see Figure 24).

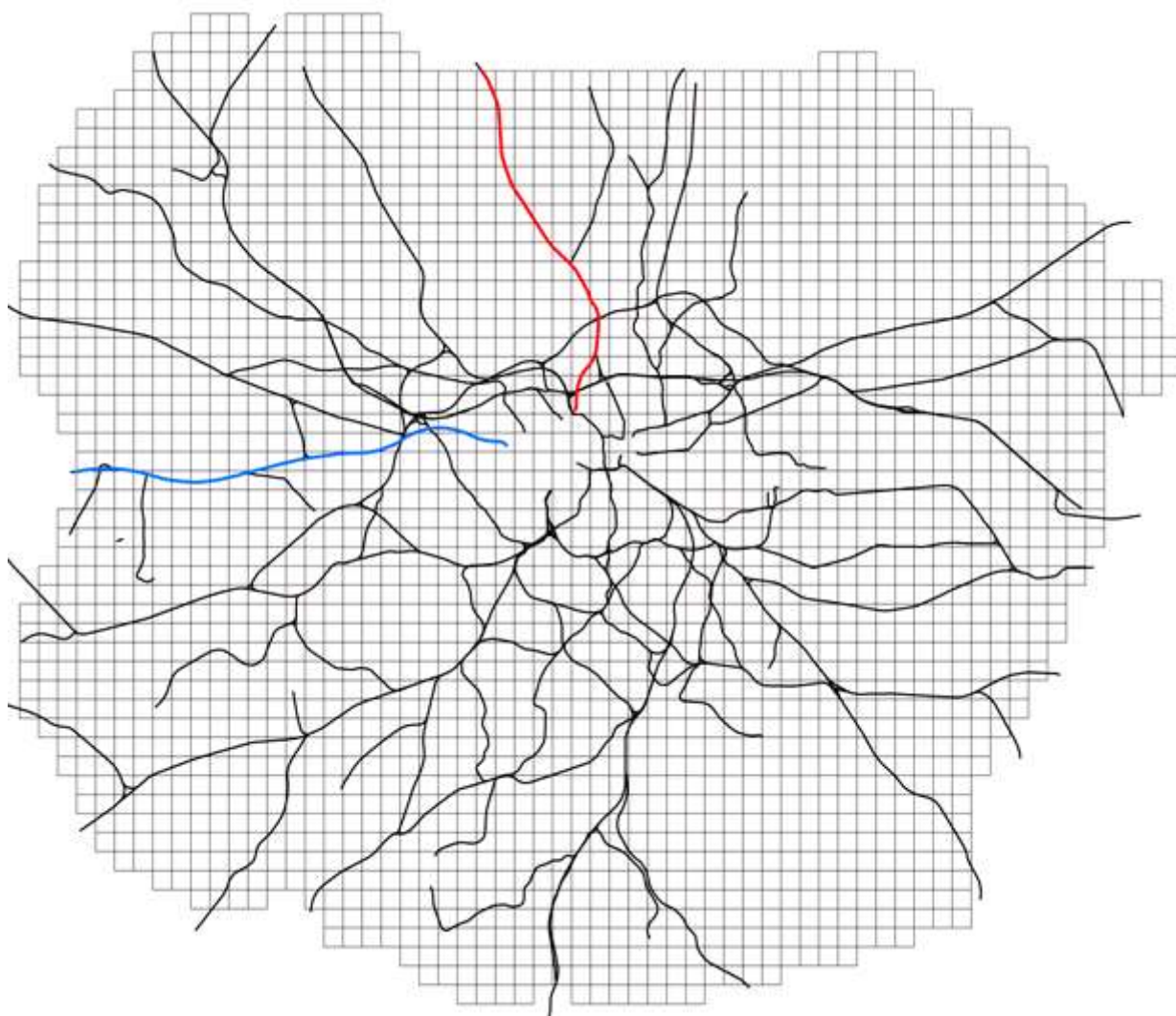


*Figure 24 National rail network (Paddington Mainline in blue and East Coast Mainline in red)*

## Activity

The train activity on Paddington and East Coast Mainlines for the rail links close to the Ealing 12 and Islington 6 monitoring site where extracted from the LAEI2008 activity data (see Table 9).

Train types	Class IC 125	Class 165 (2 Coaches)	Class 165 (3+ Coaches)	Class 66 (Freight)
Paddington link 411 (Between Southall East Jn and Southall)	78244	4669	64440	12641
East Coast link 178 (Between Finsbury Park and Holloway Sth. Jn.)	12520	503	4039	2598

Table 9 LAEI2008 annual activity on rail links 411 and 178 for different diesel train types (passenger and freight)

The train activity data along the Paddington Mainline from the LAEI2008 was compared to a 2014 sample dataset (Charles Buckingham (CB) at TfL- personal communication). Hourly train flows were calculated from each data set. As shown in

Table 10, the sample dataset indicated slightly lower activity but it was concluded that the more extensively researched LAEI2008 activity data remained appropriate.

Train types	IC 125	Class 165	Class 66 Freight
Paddington Line (CB at TfL)	10	8	2
Paddington Line (LAEI2008)	13.4	11.8	2.1

Table 10 Estimated hourly activity on the Paddington Line for different diesel train types (passenger and freight)

## New emission estimates

New emission estimates for all passenger and freight diesel train types were made for the Paddington and East Coast mainlines by combining the LAEI2008 diesel trains activity and the emission factors from the Hobson and Smith (2001) which are shown in Table 11.

EF in g/km	Class IC 125			Class 165 (2 Coaches)			Class 165 (3+ Coaches)			Class 66 (Freight)		
	NO <sub>x</sub>	CO <sub>2</sub>	PM <sub>10</sub>	NO <sub>x</sub>	CO <sub>2</sub>	PM <sub>10</sub>	NO <sub>x</sub>	CO <sub>2</sub>	PM <sub>10</sub>	NO <sub>x</sub>	CO <sub>2</sub>	PM <sub>10</sub>
	194.8	12170	17	18.6	1824	0.6	30.3	2979	1	120	19147	2.9

Table 11 Estimated emission factors for different diesel train types (passenger and freight)

By using a simple scaling factor speed, and other activity data was retained within the emission description. The recalculated total emissions were compared to the total emissions from the LAEI2010 for each mainline (see

Table 12) and a correction factor was established. The correction factors represented the ratio of the recalculated emissions over the LAEI2010 emissions. The application of emissions factors from Hobs



and Smith (2001) led to substantial reductions in the estimated NO<sub>x</sub> emissions from the both the Paddington and East Coast lines (factors of 0.30 and 0.44 respectively). Smaller corrections were found for PM<sub>10</sub> emissions (factors of 0.65 and 0.94 respectively).

	LAEI2010 NO <sub>x</sub>	Recalculated NO <sub>x</sub>	Correction factor (NO <sub>x</sub> )	LAEI2010 PM <sub>10</sub>	Recalculated PM <sub>10</sub>	Correction factor (PM <sub>10</sub> )
Paddington	1497	443	0.30	51.7	33.8	0.65
East Coast	133	59	0.44	4.9	4.6	0.94

*Table 12 Estimated total emissions in tonnes per annum and correction factor for Paddington and East Coast mainlines*

### **Model emission correction**

The correction factors from Table 12 were applied to King's LAQT model emissions input. The rail background emissions (tonnes per annum) by grid (1km x 1km) and the detailed emissions (g/km/s) by route links alongside the Paddington and East Coast mainlines were scaled by using the NO<sub>x</sub> correction factors for both NO<sub>x</sub> and primary NO<sub>2</sub> and PM<sub>10</sub> for both PM<sub>10</sub> and PM<sub>2.5</sub>. The LAEI2010 year 2010 was used as a base case and a scenario (with corrected rail) was created using the scaled railway emissions to factor existing model predictions, keeping all the other London emissions sources and model assumptions fully consistent with the LAEI2010 year 2010.

### **Model description (King's London Air Quality Toolkit, LAQT)**

King's air quality model, the London Air Quality Toolkit (LAQT), is based upon the LAEI and has provided policy support to the GLA/TfL for over 15 years. Input data contained within the London inventories have been routinely manipulated to quantify the concentration changes associated with the impacts of traffic management in support of policies such as the CCZ, WEZ, LEZ, MAQS, ORN and ULEZ.

The main LAQT capabilities highlights have been compiled below:

- The LAQT is capable of modelling all EU limit value concentrations (specifically annual mean NO<sub>x</sub>, NO<sub>2</sub>, PM<sub>10</sub>, PM<sub>2.5</sub> and PM<sub>10</sub> days > 50 µg m<sup>-3</sup>) across London, as well as incorporating detailed meteorology and urban topology.
- The LAQT includes all LAEI sources: road transport, part A/B industrial processes, gas/oil/coal, agriculture, rail, ships, airports, NRM.
- Since King's routinely produce the road transport, aviation and shipping emissions included in the LAEI, King's are in a unique position in which our LAQT seamlessly interfaces the London Inventory and as a consequence King's can be extremely flexible in the design and set up of model scenarios.
- It complies fully with DEFRA modelling requirements.

- The model produces highly detailed and spatially accurate maps of air quality, compatible with other mapping products (GIS, Mapinfo).
- A complete description of the LAQT modelling methods can be found in a recent HEI document (<http://pubs.healtheffects.org/getfile.php?u=638>).
- The LAQT has been extensively evaluated against measurements from the London Air Quality Network for all EU limit values metrics: annual mean NO<sub>x</sub>, NO<sub>2</sub>, PM<sub>10</sub>, PM<sub>2.5</sub> and PM<sub>10</sub> days > 50 µg m<sup>-3</sup>.
- The LAQT has been submitted to both phases of DEFRA's model inter-comparison exercise ([http://uk-air.defra.gov.uk/library/reports?report\\_id=654](http://uk-air.defra.gov.uk/library/reports?report_id=654)).
- The LAQT provides consistent forecasting and back-casting methods, version control, a complete audit trail of assumptions as well as complete consistency with all current GLA/TfL strategies.

The LAQT predicts London's air pollution using a kernel modelling technique to describe the initial dispersion (using ADMS dispersion algorithms). The kernel model relates to a set of model concentration fields that are produced using an emissions source of unity: either 1 g s<sup>-1</sup> (point sources), 1 g m<sup>-3</sup> s<sup>-1</sup> (volume sources) or a 1 g km<sup>-1</sup> s<sup>-1</sup> (road sources). Each kernel is created using hourly meteorological data from Heathrow Airport. The model predicts air quality in London at any point by combining the rural concentration from outside London, with London sources greater than 1 km away, using volume sources of different dimensions (2m for roads and 50m for other sources) and finally adding the contribution of local sources, less than 1 km away. The model structure enables highly detailed spatial information to be used, for example, road and rail emissions across the Greater London's transport networks, which are split into 10m sections. This allows the detailed spatial gradients in concentrations close to an emissions source to be predicted, which is where they are most important. For diesel trains, the emissions release height was taken to be 5 m. The contribution of each London source is predicted using the model kernels at every location in London across a master grid of 20m x 20m (standard resolution) and up to 5m x 5m (high resolution), allowing detailed source apportionment estimates to be made. The method for converting NO<sub>x</sub> to NO<sub>2</sub> uses well established relationships and is based upon the work of Carslaw et al. (2001), updated to include the proportion of primary NO<sub>2</sub> for each road or rail source separately. A source apportionment approach is used in predicting PM coming into London and is based upon the methods of Fuller et al. (2002) and Fuller and Green (2004, 2006).

## 8.2 Model results

The air quality modelling results was compiled and the new scenario (LAEI2010 year 2010 corrected rail) was compared with the base case (LAEI2010 year 2010). The air quality concentration maps for both the base case and scenario (with corrected rail) of NO<sub>x</sub>, NO<sub>2</sub>, PM<sub>10</sub> and PM<sub>2.5</sub> can be seen below in Figure 25 to Figure 32. With revised emissions factors, the modelled concentrations alongside the Paddington mainline shows a clear fading for NO<sub>x</sub> and NO<sub>2</sub> (70% less NO<sub>x</sub>/NO<sub>2</sub> emissions) while for PM<sub>10</sub> and PM<sub>2.5</sub>, it is less apparent due to a smaller emission reduction (35% less PM<sub>10</sub>/PM<sub>2.5</sub> emissions) and the influence of background sources for these pollutants.

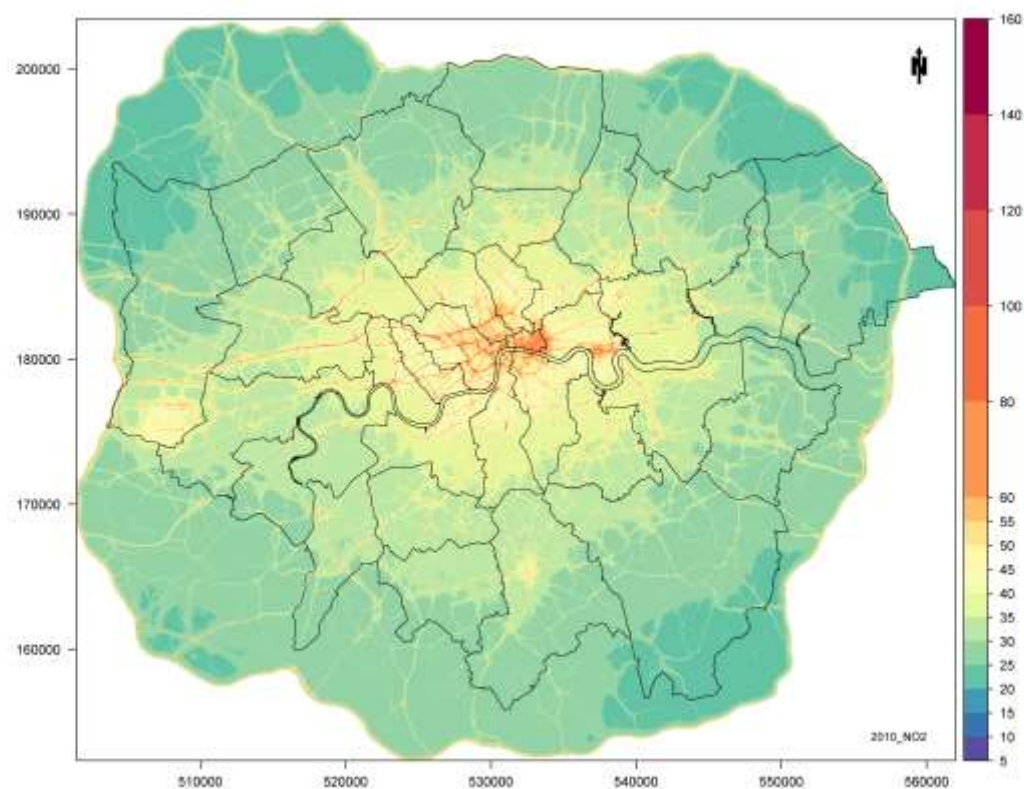


Figure 25 Annual mean NO<sub>2</sub> concentrations ( $\mu\text{g m}^{-3}$ ) in 2010 for the LAEI2010 base case

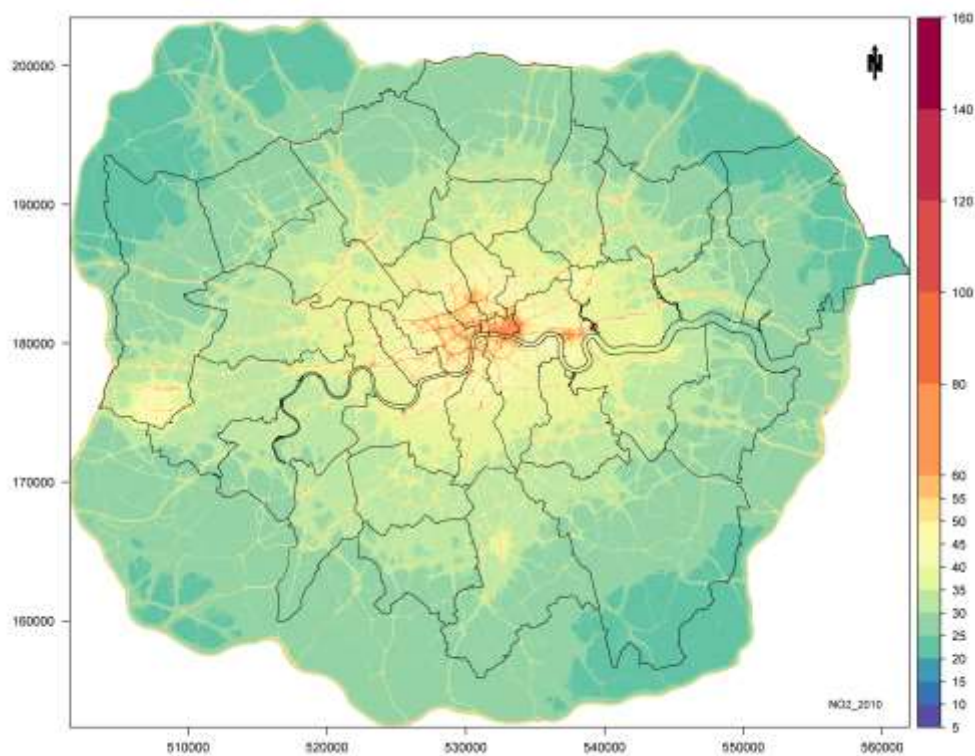


Figure 26 Annual mean NO<sub>2</sub> concentrations ( $\mu\text{g m}^{-3}$ ) in 2010 for the corrected rail scenario

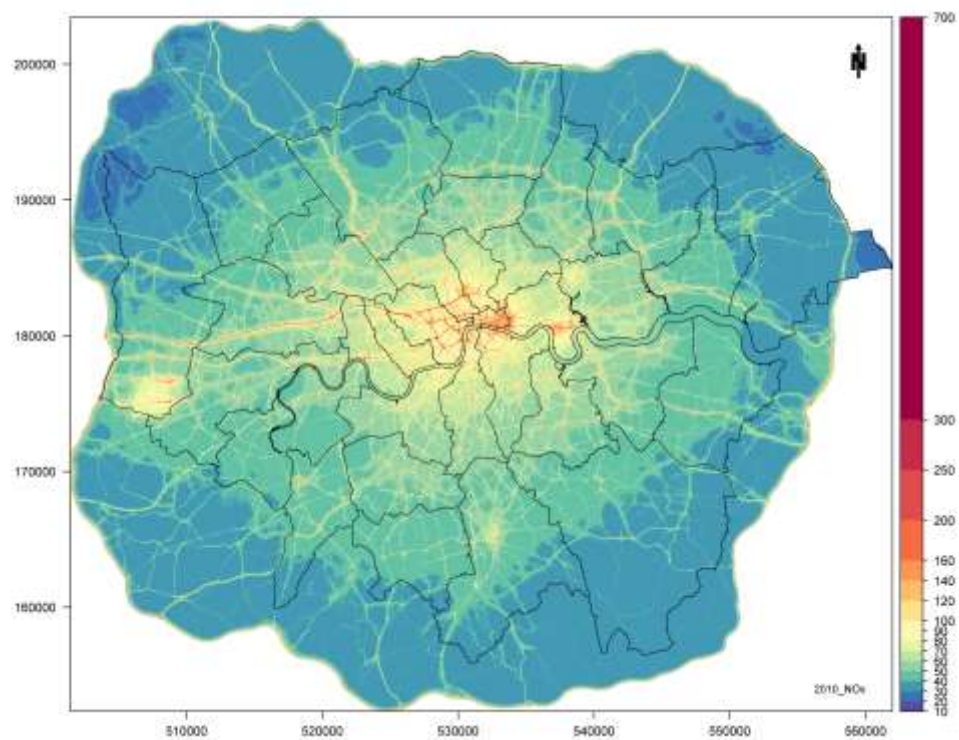


Figure 27 Annual mean NO<sub>x</sub> concentrations ( $\mu\text{g m}^{-3}$ ) in 2010 for the LAEI2010 base case

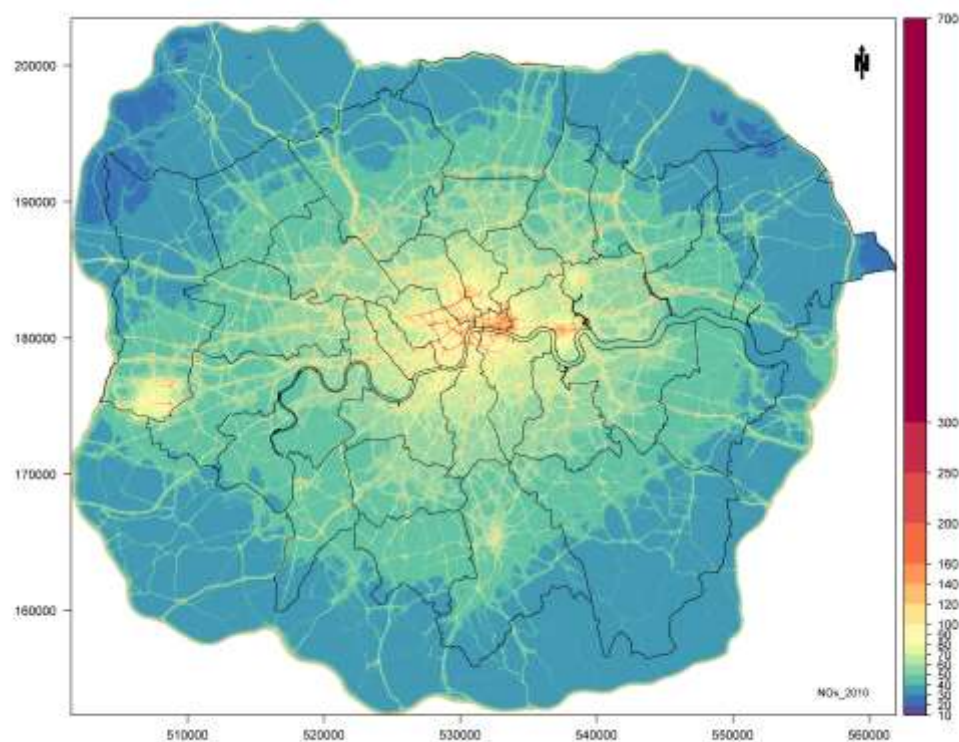


Figure 28 Annual mean NO<sub>x</sub> concentrations ( $\mu\text{g m}^{-3}$ ) in 2010 for the corrected rail scenario



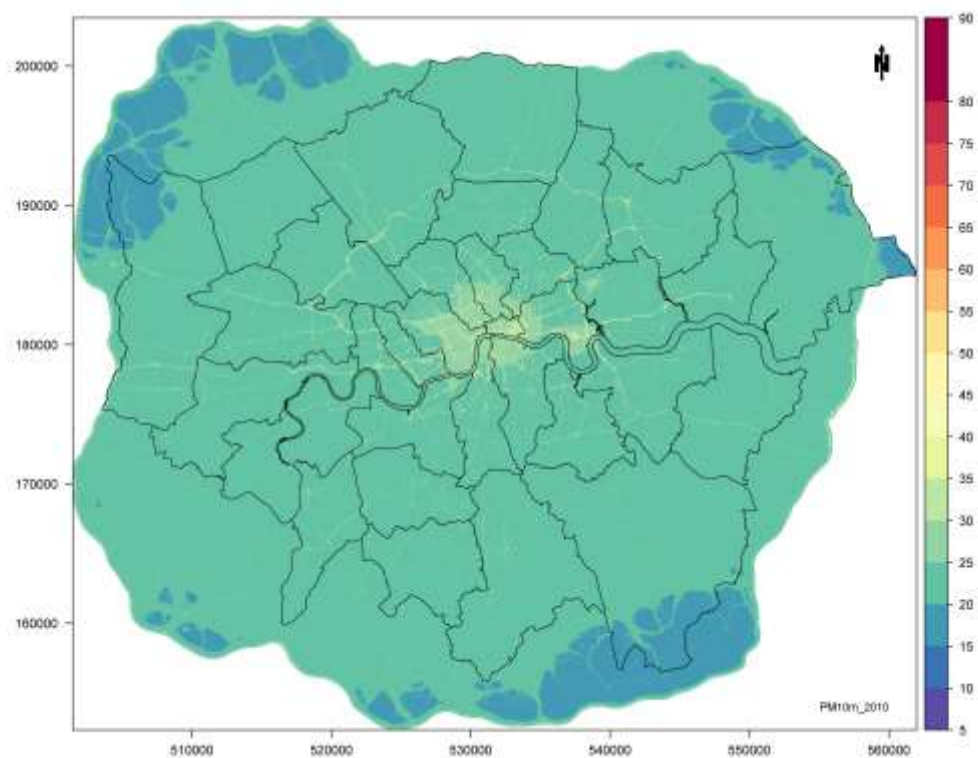


Figure 29 Annual mean  $PM_{10}$  concentrations ( $\mu g m^{-3}$ ) in 2010 for the LAEI2010 base case

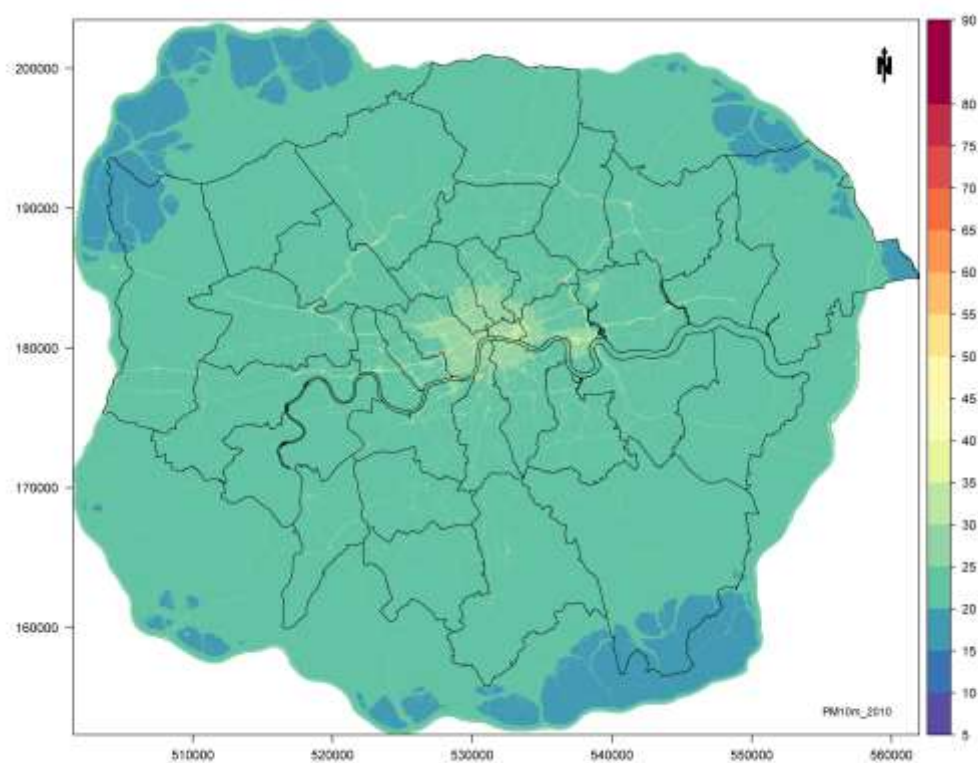


Figure 30 Annual mean  $PM_{10}$  concentrations ( $\mu g m^{-3}$ ) in 2010 for the corrected rail scenario

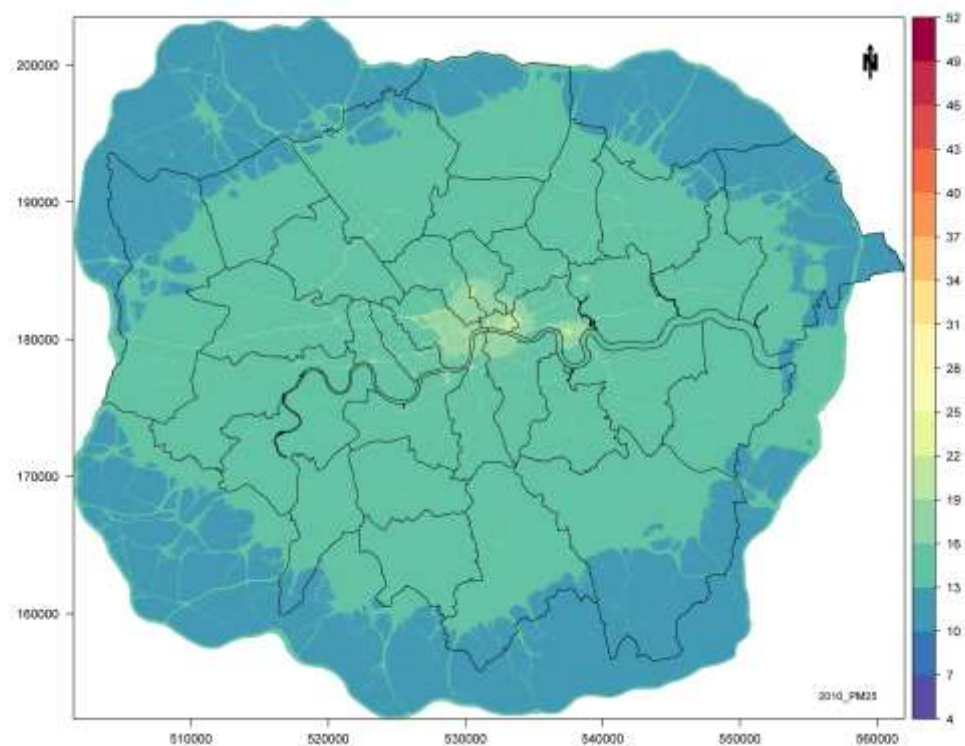


Figure 31 Annual mean PM<sub>2.5</sub> concentrations ( $\mu\text{g m}^{-3}$ ) in 2010 for the LAEI2010 base case

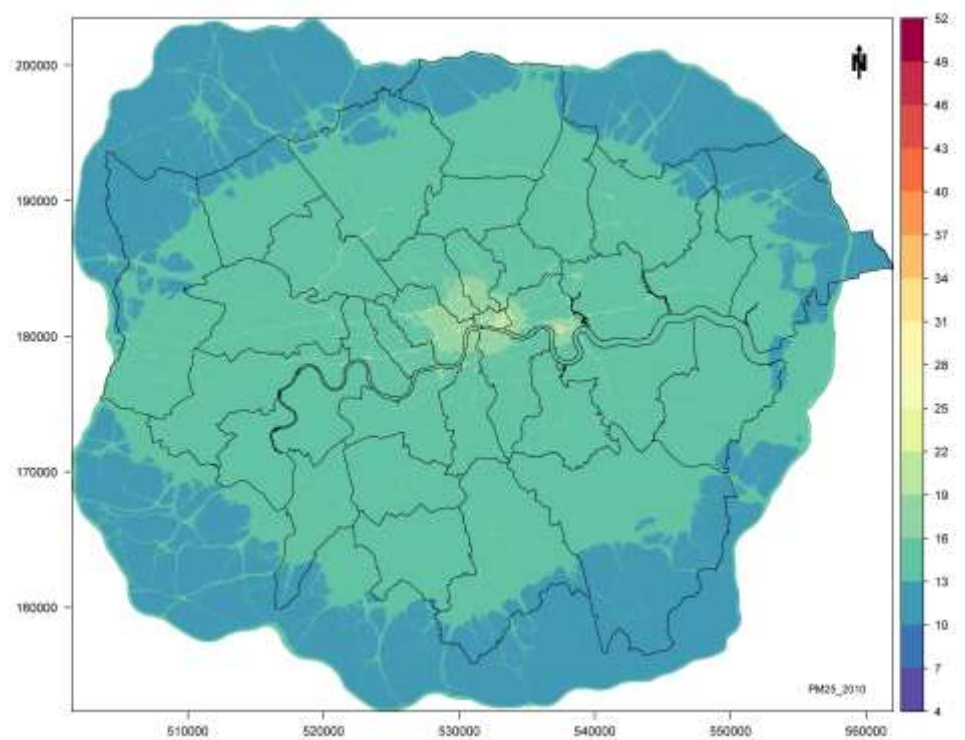


Figure 32 Annual mean PM<sub>2.5</sub> concentrations ( $\mu\text{g m}^{-3}$ ) in 2010 for the corrected rail scenario

The new scenario (LAEI2010 year 2010 corrected rail) modelling results were interpolated and compared to the measurements using LAQN sites and diffusion tube measurements (see Table 13). Figure 5 and Figure 6 (earlier) show the location of the measurement sites chosen alongside the Paddington and East Coast mainlines.

A scatter plot of NO<sub>2</sub> measurements versus both the base case (LAEI2010 year 2010) and the new scenario (LAEI2010 year 2010 corrected rail) modelled results can be found in

Figure 33. Table 13 and

Figure 33 clearly show that the new modelling scenario with the corrected emission for the Paddington and King's Cross mainlines showed an improved agreement with the measurements and that concentrations at these a points were below the annual mean limit values at the majority of the measurement sites.

The modelled NO<sub>x</sub> concentration was lower in the corrected scenario where compared to the base case. When comparing the corrected model results to the measurements it was found that the corrected model results were 20% less than the measured concentrations at Ealing but around 15% greater than the measured concentrations Islington. Caution needs to be applied when interpreting the results from two measurement points only but the comparison between modelled and measured NO<sub>x</sub> could be indicative uncertainty in the NO<sub>x</sub> prediction but suggests that any overall bias might be small. Only small changes are apparent between the base and corrected cases for PM<sub>10</sub> and it is difficult to draw conclusions on these.

Rail line	Pollutant	Site	Measured			Modelled Base case Year 2010 LAEI2010	Modelled Scenario Year 2010 Rail corrected	Change (Base case vs scenario)
			2010	2011	2012			
Paddington	NO <sub>x</sub>	EI2		84.6	88.3	111.9	67.9	-39.31%
Paddington	NO <sub>2</sub>	EI2		34.4	35.6	49.5	37.9	-23.52%
Paddington	NO <sub>2</sub>	6			34.5	46.1	37.0	-19.74%
Paddington	NO <sub>2</sub>	7			37.1	49.8	37.9	-23.95%
Paddington	NO <sub>2</sub>	22			37.7	52.3	39.9	-23.74%
Paddington	NO <sub>2</sub>	23			39.1	49.5	37.9	-23.52%
Paddington	NO <sub>2</sub>	97			39.5	52.3	44.9	-14.26%
Paddington	NO <sub>2</sub>	98			38.8	58.1	45.2	-22.27%
Paddington	PM <sub>10</sub>	EI2		21.8	22.9	23.4	22.8	-2.43%
East Coast	NO <sub>x</sub>	IS6	55.0	56.2	56.9	66.4	65.2	-1.81%
East Coast	NO <sub>2</sub>	IS6	36.9	36.7	36.5	40.0	39.6	-1.13%
East Coast	NO <sub>2</sub>	AG1			37.0	39.9	39.4	-1.28%
East Coast	NO <sub>2</sub>	AG2			38.0	39.8	39.4	-1.09%
East Coast	PM <sub>10</sub>	IS6	21.5	22.4	24.1	24.0	24.0	-0.05%

Table 13 Measured and modelled annual concentration (in  $\mu\text{g m}^{-3}$ ) at LAQN and diffusion tube sites alongside the Paddington and East Coast Mainlines.



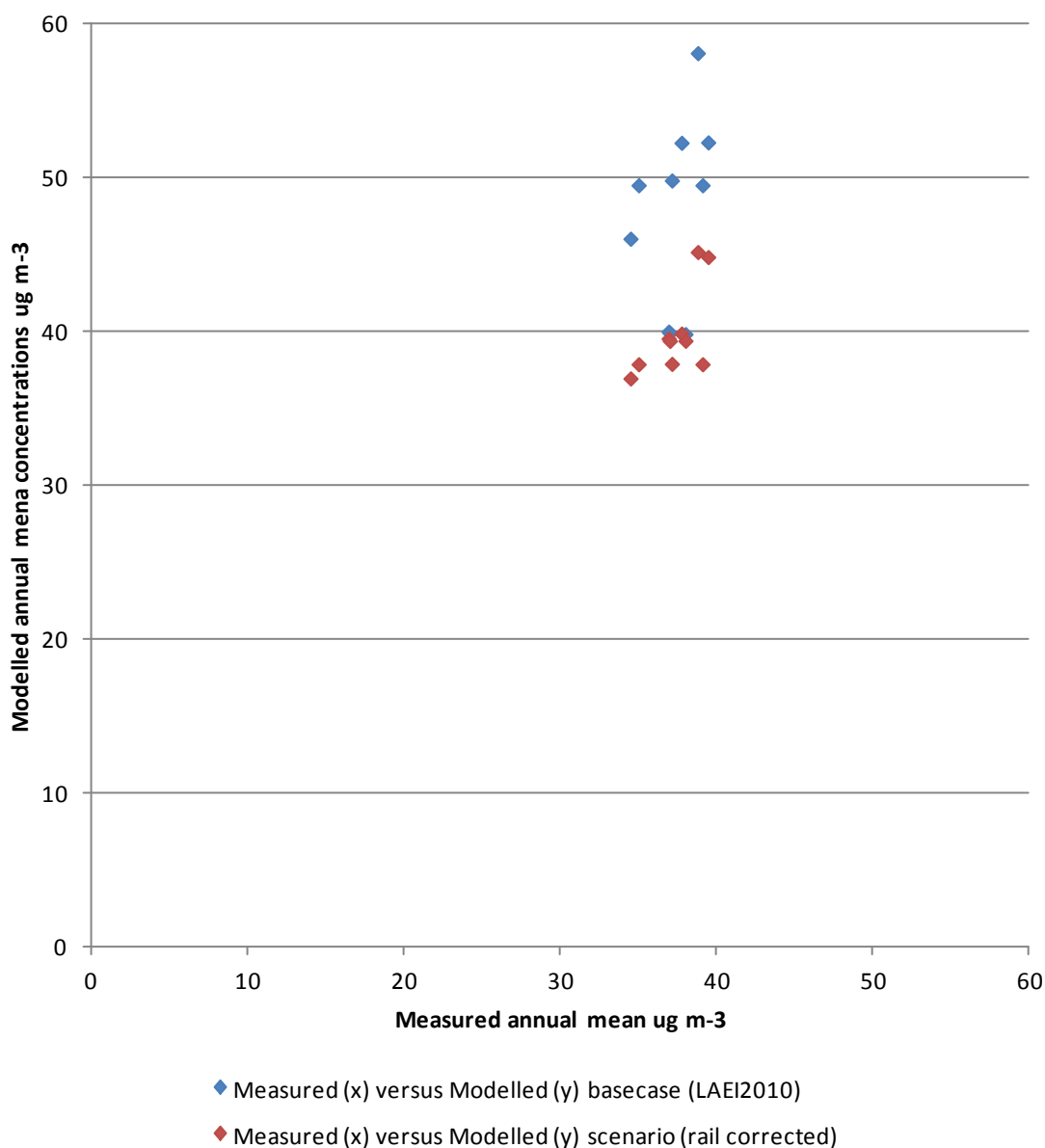


Figure 33 Measured (x-axis) versus modelled (y-axis)  $\text{NO}_2$  concentration (in  $\mu\text{g}/\text{m}^3$ ) for the base case (LAEI2010) and the scenario (rail corrected) in 2010.

Focusing on Ealing and Islington, comparing the modelled outputs in Figure 34 to those in Figure 2, a clear decrease in  $\text{NO}_2$  is apparent around the Paddington Mainline. The smaller change in modelled concentrations is less apparent on the East Coast Mainline.



Figure 34 Modelled annual mean  $\text{NO}_2$  concentration for 2010. Left panel shows west London with the Paddington Mainline indicated by an arrow. The right panel shows inner north London with the East Coast Mainline indicated with an arrow. Areas shaded in yellow and to to red exceed the EU Limit Value of  $40 \mu\text{g m}^{-3}$

## 9 Conclusions

In contrast to expectations from modelled data the annual mean  $\text{NO}_2$  concentration at Ealing 12 was less than the AQS objective and EU Limit Value concentration of  $40 \mu\text{g m}^{-3}$  and no increment in  $\text{NO}_2$  was found over that measured 600 m from the railway line. The maximum hourly mean  $\text{NO}_2$  concentration at Ealing 12 was less than the threshold for the short-term EU Limit Value concentration for  $\text{NO}_2$  ( $200 \mu\text{g m}^{-3}$ ). Small increments were found in the concentrations of  $\text{NO}_x$ ,  $\text{PM}_{10}$  and BC.

Islington 6 experienced greater concentrations than those measured at background for all pollutants. Again, in contrast to expectations from modelled data the annual mean concentration at Islington 6 was less than the AQS objective and EU Limit Value concentration of  $40 \mu\text{g m}^{-3}$ . The maximum hourly mean  $\text{NO}_2$  concentration at Islington 6 exceeded the EU short term limit value during periods of poor pollutant dispersion when many London sites also experienced pollutant similar concentrations suggesting that local sources where not responsible.

It must be emphasised that the high  $\text{NO}_x$  and  $\text{NO}_2$  concentrations predicted by modelling were not found in ambient measurements at either railway location. The presence of  $\text{NO}_2$  concentrations below the annual Limit Value were supported by diffusion tube measurements. The paired diffusion tubes placed either side of the Paddington Mainline also showed no evidence of a strong  $\text{NO}_2$  emissions from the diesel trains.

Correlations between PM chemical composition measurements at both railway sites showed a mixture of particles from brake wear from traffic and only weak evidence of a separate rail source.

The later source was more resolved when the increment in concentrations over background was considered.

Two tracer methods were used to estimate the expected Fe that might be due to rail track wear. Using BC measurements as a tracer to account for traffic activity, a track wear contribution of around  $1 \mu\text{g m}^{-3}$  ( $\text{Fe}_2\text{O}_3$ ) was estimated at both Ealing 12 and Islington 6. This agreed well with Gehrig et al 2007 who found track wear contributions of around  $1.5 \mu\text{g m}^{-3}$   $\text{Fe}_2\text{O}_3$  at a similar distance from a busy rail line ( $\sim 10$  m) along with close correlations between Fe and Mn reflecting rail composition. An alternative approach using Ba as a tracer to account for brake wear provided lower track wear estimates; a concentration of around  $0.2 \mu\text{g m}^{-3}$  ( $\text{Fe}_2\text{O}_3$ ). In conclusion there is weak evidence of Fe from track wear alongside the two railway sites but this source was too small to be separated from and from traffic brake wear and accurate quantification was not possible. Unlike Gehrig et al (2007), due to the urban nature of our measurements, the clear dominance of brake wear to Cu prevented a calculation of the local Cu concentration from train conductor wear.

It was possible to discern an increment in  $\text{NO}_x$  and  $\text{CO}_2$  concentrations at Ealing 12 to the south/east, consistent with there being a source(s) in the direction of the railway. The  $\text{CO}_2$  and  $\text{NO}_x$  concentrations at Ealing were are noisy but it was possible to quantify ratios of  $\text{NO}_x/\text{CO}_2$  of around 0.0025, which were typical of a road source and consistent with traffic vehicle emission remote sensing. The noisy nature of the results, particularly compared to a major road such as Marylebone Road suggests that the rail source is not large at this location and cannot be separated from road traffic diesel. At Islington 6 the  $\text{NO}_x/\text{CO}_2$  were consistent with a road traffic source dominated by light duty vehicles. A clear  $\text{NO}_2$  source was present to the SSW of the site but this could not be determined. In summary, although the detection of a diesel train sources of  $\text{NO}_x$  and  $\text{PM}_{10}$  was hampered by surrounding traffic sources the absence of a clear diesel train source demonstrates that diesel trains were not the dominant sources of  $\text{NO}_x$ ,  $\text{NO}_2$  or  $\text{PM}_{10}$  at these locations. Measurements from Ealing suggested that the  $\text{NO}_x$ , PM and  $\text{CO}_2$  emissions ratios from diesel trains are likely to be consistent with unabated diesel vehicles.

One possibility for the lack of a clear  $\text{NO}_x$  signal at the Ealing 12 site is that the site was located too close to the railway and the plumes from the diesel trains were above the site itself. However, we do not consider this to be the case. First, there was also no evidence of a clear  $\text{NO}_x$  source at the Ealing 7 background site, which might be expected at that distance from the track. Second, the polar plots show no evidence of the presence of an elevated plume, which would tend to be brought quickly down to ground level at high wind speeds (similar to the behaviour of chimney stack emissions). Finally, the Burchill et al (2011) work suggests that plumes from fast-moving diesel trains are very rapidly mixed due to the highly turbulent flow brought about by the moving trains.

The absence of a clear signal from train emissions prevented the derivation of new emission factors from the ambient measurements as originally intended. Instead emissions factor from Hobson and Smith (2001) were selected as an alternative to those used in the current LAEI. These emission factors were combined with train activity to factor the existing LAEI emissions to remodel the Paddington and East Coast Mainlines. With revised factors decreased modelled emissions alongside the Paddington mainline by 70% for  $\text{NO}_x$  and 35% for  $\text{PM}_{10}/\text{PM}_{2.5}$  emissions. Smaller changes were found

for emissions alongside the East Coast Mainline where  $\text{NO}_x$  emissions were modelled to be 66% lower and PM emissions decreased by 6%.

Using these new emission calculations the model predictions for Paddington and King's Cross mainlines showed an improved agreement with the measurements and that concentrations at these points were below the annual mean limit values at the majority of the measurement sites. Small changes are apparent between the base and corrected cases for  $\text{PM}_{10}$ .

In summary the difference between the initial modelled concentrations with large areas exceeding the  $\text{NO}_2$  limit values was not supported by measurements. It was difficult to detect a clear pollution signal from the railways in terms of  $\text{NO}_x$ ,  $\text{NO}_2$ , PM and PM metals. It is possible the detection of emissions from the railways was confounded by other urban sources but it is clear from this study that diesel trains do not make a large contribution to urban air quality in London. This finding has clear implications for local air quality management priorities in Ealing and Islington and other local authorities with diesel train lines. Air quality actions plans in Ealing and Islington should be revised accordingly. Both Ealing and Islington have declared air quality management areas (AQMA) that cover the whole borough. Given that these areas were not dependent on the railway source alone it is unlikely that the boundaries of the AQMS will require revision.

## 10 Recommendations for further research

Without this measurement study large resources could have been expended to abate pollution emissions from diesel trains. This raises important issues for emissions inventory compilation. Although concentration models are routinely "validated" by comparison to measured concentrations, this is normally undertaken for typical roadside and background concentrations without focus on specific emission sources. The amendment or introduction of emission sources needs to be verified against real-world measurements before being used in air quality and policy assessments.

Although the revised emission factors appear more consistent with measured concentrations it should be noted that these date from the late 1990s. New emission factors are clearly required for the newer types of diesel train being operated on the UK's railways.

The derivation of real-world emissions factors was hampered by the relatively small size of the railways emissions compared to other urban sources of air pollution. A study alongside busy railways in a rural environment would provide a better opportunity to quantify railway emissions.

## 11 Acknowledgments

We would like to extend out thanks to the following:

Rizwan Yunus, London Borough of Ealing, for installing the Ealing – Southall monitoring site, for the diffusion tube and other measurements and comments on the project report.

John Freeman, London Borough of Ealing for support with the project design and comments on the project report and for the original application and project management.

Sukky Choongh-Campbell and Paul Clift for diffusion tube measurements in Islington and their support with the original application and project management.

Charles Buckingham, Transport for London, for train activity data and supporting information.

Timothy Baker, King's College London for leading the monitoring site work including the installation of partisol and black carbon measurements.

Max Priestman, King's College London for CO<sub>2</sub> measurements.

Monica Pirani, King's College London, for additional site visits during the black carbon measurement campaigns at Ealing Southall.

Anja Tremper, David Green and Andrew Cakebread, King's College London,  
for PM metals measurements.

Anna Font, King's College London for "Cosemans" plots of metals concentrations.

Defra, the London Boroughs of Ealing, Islington and Tower Hamlets, Transport for London, the Medical Research Council and National Environment research council for funding the project and other measurement programmes in London without which this work would not have been possible.

## 12 References

- BIPM, IEC, IFCC, ILAC, ISO, IUPAC, IUPAP and OIML, (2008). Evaluation of measurement data - Guide to the expression of uncertainty in measurement. On line at:  
[http://www.bipm.org/utis/common/documents/jcgm/JCGM\\_100\\_2008\\_E.pdf](http://www.bipm.org/utis/common/documents/jcgm/JCGM_100_2008_E.pdf)
- Butterfield, B., Beccaceci, S., Quincey, P., Sweeney, B., Whiteside, K., Fuller, G., Green, D., Font Font, A., (2013). 2012 Annual Report for the UK Black Carbon Network. National Physical Laboratory, Teddington on line at [http://uk-air.defra.gov.uk/assets/documents/reports/cat13/1309060901\\_2012\\_BC\\_Network\\_Annual\\_Report-Final.pdf](http://uk-air.defra.gov.uk/assets/documents/reports/cat13/1309060901_2012_BC_Network_Annual_Report-Final.pdf)
- Bek, B.H, Sorenson, S.C, 1999. Future emissions from railway traffic. Technical University of Denmark, Lyngby, Denmark.
- Bentley, S.T. (2004) Graphical techniques for constraining estimates of aerosol emissions from motor vehicles using air monitoring network data. Atmospheric Environment, Volume 38, Issue 10, Pages 1491-1500.
- Burchill, M. J., Gramotnev, D. K., Gramotnev, G., Davison, B. M., & Flegg, M. B. (2011). Monitoring and analysis of combustion aerosol emissions from fast moving diesel trains. Science of the total environment, 409(5), 985-993.
- Bukowiecki, N., Gehrig, R., Hill, M., Lienemann, P., Zwicky, C. N., Buchmann, B., ... & Baltensperger, U. (2007). Iron, manganese and copper emitted by cargo and passenger trains in Zürich (Switzerland): size-segregated mass concentrations in ambient air. Atmospheric environment, 41(4), 878-889.
- Carslaw, D. C., Beevers, S. D., & Fuller, G. (2001). An empirical approach for the prediction of annual mean nitrogen dioxide concentrations in London. Atmospheric Environment, 35(8), 1505-1515.
- Carslaw, D. C., Beevers, S. D., Ropkins, K., & Bell, M. C. (2006). Detecting and quantifying aircraft and other on-airport contributions to ambient nitrogen oxides in the vicinity of a large international airport. Atmospheric Environment, 40(28), 5424-5434.
- Carslaw, D.C. and Rhys-Tyler, G. (2013). New insights from comprehensive on-road measurements of NO<sub>x</sub>, NO<sub>2</sub> and NH<sub>3</sub> from vehicle emission remote sensing in London, UK. Atmospheric Environment, Vol. 81 339-347.
- Cosemans, G., Kretzschmar, J., Mensink, C., (2008). Pollutant roses for daily averaged ambient air pollutant concentrations, Atmospheric Environment, 42, (29), 6982-6991.
- Fuller, G. W., Carslaw, D. C., & Lodge, H. W. (2002). An empirical approach for the prediction of daily mean PM<sub>10</sub> concentrations. Atmospheric Environment, 36(9), 1431-1441.
- Fuller, G. W., & Green, D. (2006). Evidence for increasing concentrations of primary PM<sub>10</sub> in London. Atmospheric Environment, 40(32), 6134-6145.

Gehrig, R., Hill, M., Lienemann, P., Zwicky, C. N., Bukowiecki, N., Weingartner, E., ... & Buchmann, B. (2007). Contribution of railway traffic to local PM<sub>10</sub> concentrations in Switzerland. *Atmospheric Environment*, 41(5), 923-933.

Green, D. C., Fuller, G. W., & Baker, T. (2009). Development and validation of the volatile correction model for PM<sub>10</sub>—An empirical method for adjusting TEOM measurements for their loss of volatile particulate matter. *Atmospheric Environment*, 43(13), 2132-2141.

Hobson, M., Smith, A., 2001. Rail emission model. AEA Technology, Culham.

Jones, A. M., & Harrison, R. M. (2006). Assessment of natural components of PM<sub>10</sub> at UK urban and rural sites. *Atmospheric Environment*, 40(40), 7733-7741.

Jorgensen, M.W., Sorenson, S.C., (1997). Estimating emissions from railway traffic. Technical University of Denmark, Lyngby, Denmark.

Lenschow, P., Abraham, H. J., Kutzner, K., Lutz, M., Preuß, J. D., & Reichenbacher, W. (2001). Some ideas about the sources of PM<sub>10</sub>. *Atmospheric Environment*, 35, S23-S33.

Lorenzo, R., Kaegi, R., Gehrig, R., & Grobety, B. (2006). Particle emissions of a railway line determined by detailed single particle analysis. *Atmospheric Environment*, 40(40), 7831-7841.

Park, S. S., Hansen, A. D., & Cho, S. Y. (2010). Measurement of real time black carbon for investigating spot loading effects of Aethalometer data. *Atmospheric Environment*, 44(11), 1449-1455.

Sawant, A. A., Nigam, A., Miller, J. W., Johnson, K. C., & Cocker, D. R. (2007). Regulated and non-regulated emissions from in-use diesel-electric switching locomotives. *Environmental science & technology*, 41(17), 6074-6083.

Thorpe, A., & Harrison, R. M. (2008). Sources and properties of non-exhaust particulate matter from road traffic: a review. *Science of the total environment*, 400(1), 270-282.

Virkkula, A., Mäkelä, T., Hillamo, R., Yli-Tuomi, T., Hirsikko, A., Hämeri, K., & Koponen, I. K. (2007). A simple procedure for correcting loading effects of aethalometer data. *Journal of the Air & Waste Management Association*, 57(10), 1214-1222.